Platinum Group Thiophenoxyimine Complexes: Syntheses and Crystallographic/Computational Studies

Jamin L. Krinsky, John Arnold,* and Robert G. Bergman*

Department of Chemistry, University of California, Berkeley, California, 94720

Received October 3, 2006

Monomeric thiosalicylaldiminate complexes of rhodium(I) and iridium(I) were prepared by ligand transfer from the homoleptic zinc(II) species. In the presence of strongly donating ligands, the iridium complexes undergo insertion of the metal into the imine carbon−hydrogen bond. Thiophenoxyketimines were prepared by nontemplated reaction of *o*-mercaptoacetophenone with anilines and were complexed with rhodium(I), iridium(I), nickel(II), and platinum(II). X-ray crystallographic studies showed that while the thiosalicylaldiminate complexes display planar ligand conformations, those of the thiophenoxyketiminates are strongly distorted. Results of a computational study predicted that all synthetically accessible thiophenoxyketiminates will display distorted geometries.

Introduction

Transition metal complexes bearing salicylaldiminate ligands have been employed successfully in a wide variety of catalytic systems. Research regarding this ligand class has been greatly facilitated by their ease of synthesis: A large range of structures can be accessed, often requiring only one synthetic step from the many commercially available salicylaldehydes and amines (eq 1). Jacobsen et al. have developed a highly efficient olefin

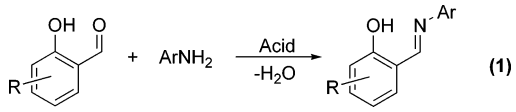

(1)

epoxidation system employing a tetradentate (salen-type) derivative (Figure 1a).[1] Titanium and zirconium complexes of bidentate salicylaldiminates have proven to be extremely active catalysts in the production of polyolefins.[2] Grubbs and others have further extended the utility of these ligands with respect to olefin polymerization, developing neutral, functional-group-tolerant nickel catalysts (Figure 1b).[3] These late transition metal catalysts, however, tend to undergo deactivating ligand redistribution reactions unless very sterically demanding salicylaldiminates are used.[4] Examples of heavier platinum-group metal complexes are present in the literature,[5] and some small-molecule reactivity has been explored.[6] However, ligand lability of the bidentate salicylaldiminates has limited their utility as supporting ligands.[7]

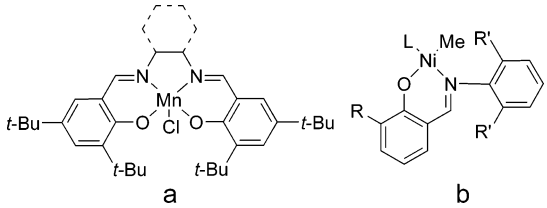

Figure 1. a. Jacobsen epoxidation catalyst (salen-type ligand) b. Olefin polymerization catalyst (bidentate salicylaldiminate ligand).

In place of the phenolate functionality of salicylaldiminates, thiosalicylaldiminates possess a thiophenolate moiety which might be expected to form a relatively inert bond with soft, polarizable metals. Homoleptic, first-row transition and main-group element complexes are known for iron through copper and the zinc triad, and incorporate bidentate, tridentate, and tetradentate ligand variants;[8] in addition, a few palladium species have been prepared.[9] While these complexes have been known for some time, their behavior as supporting ligands during metal-centered transformations is largely unexplored.[10] A major obstacle to their investigation has been the instability[11] of free

(1) Jacobsen, E. N.; Zhang, W.; Muci, A. R.; Ecker, J. R.; Deng, L. *J. Am. Chem. Soc.* **1991**, *113*, 7063−7064.

(2) (a) Matsui, S.; Mitani, M.; Saito, J.; Tohi, Y.; Makio, H.; Matsukawa, N.; Takagi, Y.; Tsuru, K.; Nitabaru, M.; Nakano, T.; Tanaka, H.; Kashiwa, N.; Fujita, T. *J. Am. Chem. Soc.* **2001**, *123*, *6847*−6856; (b) Mitani, M.; Furuyama, R.; Mohri, J.; Saito, J.; Ishii, S.; Terao, H.; Kashiwa, N.; Fujita, T. *J. Am. Chem. Soc.* **2002**, *124*, 7888−7889; (c) Hustad, P. D.; Coates, G. W. *J. Am. Chem. Soc.* **2002**, *124*, 11578−11579.

(3) (a) Wang, C. M.; Friedrich, S.; Younkin, T. R.; Li, R. T.; Grubbs, R. H.; Bansleben, D. A.; Day, M. W. *Organometallics* **1998**, *17*, 3149−3151; (b) Younkin, T. R.; Conner, E. F.; Henderson, J. I.; Friedrich, S. K.; Grubbs, R. H.; Bansleben, D. A. *Science* **2000**, *287*, 460−462.

(4) Connor, E. F.; Younkin, T. R.; Henderson, J. I.; Waltman, A. W.; Grubbs, R. H. *Chem. Commun.* **2003**, 2272−2273.

(5) (a) Kerber, W. D.; Nelsen, D. L.; White, P. S.; Gagne, M. R. *Dalton* **2005**, 1948−1951; (b) Alteparmakian, V.; Robinson, S. D. *Inorg. Chim. Acta* **1986**, *116*, L37−L38; (c) Leipoldt, J. G.; Basson, S. S.; Grobler, E. C.; Roodt, A. *Inorg. Chim. Acta* **1985**, *99*, 13−17; (d) Bonnaire, R.; Potvin, C.; Manoli, J. M. *Inorg. Chim. Acta* **1980**, *45*, L255−L256.

(6) (a) Chatterjee, D.; Mitra, A.; Roy, B. C. *React. Kinet. Catal. Lett.* **2000**, *70*, 147−151; (b) Anderson, D. J.; Eisenberg, R. *Organometallics* **1996**, *15*, 1697−1706; (c) El-Hendawy, A. M.; Alkubaisi, A. H.; El-Kourashy, A. E.; Shanab, M. M. *Polyhedron* **1993**, *12*, 2343−2350; (d) Pasini, A.; Caldirola, C.; Colombo, A.; Ghilotti, M. J. *Organomet. Chem.* **1988**, *345*, 201−208.

(7) (a) Sariego, R.; Carkovic, I.; Martinez, M. *Transition Met. Chem.* **1984**, *9*, 106−108; (b) Mague, J. T.; Nutt, M. O. J. *Organomet. Chem.* **1979**, *166*, 63−77.

(8) (a) Marin-Becerra, A.; Stenson, P. A.; McMaster, J.; Blake, A. J.; Wilson, C.; Schroder, M. *Eur. J. Inorg. Chem.* **2003**, 2389−2392; (b) Kaasjager, V. E.; Puglisi, L.; Bouwman, E.; Driessen, W. L.; Reedijk, J. *Inorg. Chim. Acta* **2000**, *310*, 183−190; (c) Mugesh, G.; Singh, H. B.; Butcher, R. J. *Eur. J. Inorg. Chem.* **1999**, 1229−1236; (d) Goswami, N.; Eichhorn, D. M. *Inorg. Chem.* **1999**, *38*, 4329−4333; (e) Marini, P. J.; Berry, K. J.; Murray, K. S.; West, B. O.; Irving, M.; Clark, P. E. *J. Chem. Soc., Dalton Trans.* **1983**, 879−884.

(9) (a) Hoskins, B. F.; Robson, R.; Williams, G. A.; Wilson, J. C. *Inorg. Chem.* **1991**, *30*, 4160−4166; (b) Hoskins, B. F.; McKenzie, C. J.; Robson, R.; Lu, Z. R. *J. Chem. Soc., Dalton Trans.* **1990**, 2637−2641.

10.1021/om0609057 CCC: $37.00
Publication on Web 01/17/2007

Scheme 1

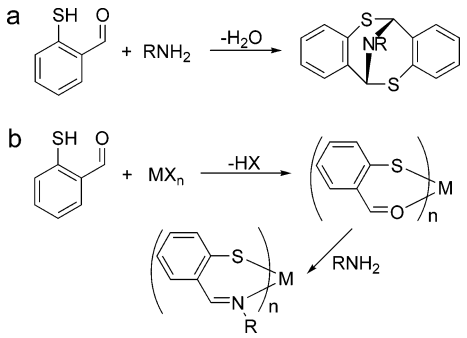

Scheme 2

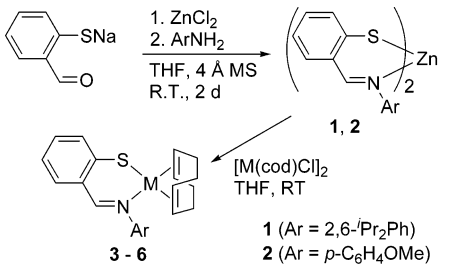

3 (M = Rh, Ar = 2,6-^{i}Pr$_2$Ph); **4** (M = Ir, Ar = 2,6-^{i}Pr$_2$Ph)
5 (M = Rh, Ar = *p*-C$_6$H$_4$OMe); **6** (M = Ir, Ar = *p*-C$_6$H$_4$OMe)

thiosalicylaldimines: condensation of 2-mercaptobenzaldehyde with amines frequently results in the formation of dithiocin derivatives (Scheme 1a).[12] This limitation can be overcome using a templated synthetic approach wherein a preformed metal−aldehyde complex is treated with the appropriate amine (Scheme 1b).[13] However, the approach is limited to cases where the metal−aldehyde complex precursor is stable, which we have found excludes the second- and third-row platinum group metals in low oxidation states. Reported herein are rational synthetic routes to heteroleptic thiosalicylaldiminate and thiophenoxyketimine complexes of rhodium, iridium, nickel, and platinum. The first two sections describe the synthesis and reactivity of new thiosalicylaldiminate complexes and highlight some issues of ligand stability. Sections 3 through 5 concern the preparation of more robust thiophenoxyketimines, their complexation with transition metal synthons, and some ligand substitution chemistry of the resulting complexes. Following that is a crystallographic/computational study that correlates ligand steric factors with their coordination behavior. Finally, a modified aryl thiophenoxyketimine is presented which displays a striking flexibility in its metal-coordination chemistry.

Results and Discussion

1. Preparation and Structural Properties of Thiosalicylaldiminate Complexes. Early in our investigations it became evident that established synthetic routes are not amenable to the preparation of late transition metal thiosalicylaldiminate complexes. Treatment of dichlorobis(1,5-cyclooctadiene)diiridium with sodium 2-formylbenzenethiolate resulted in a product mixture that appeared by ^{1}H NMR to contain the desired iridium thiolate. However, this species decomposed over 1 h at ambient temperature in solution, precluding its use as a synthon for further elaboration. Since the templated syntheses of the desired ligands were already proven effective when starting from the stable homoleptic zinc(II) aldehyde complexes,[14] it was postulated that reaction of thiosalicylaldiminate zinc species with platinum-group chlorides might provide an alternate synthetic route, much as dialkylzinc reagents alkylate platinum group chlorides (Scheme 2). Indeed, the bis(thiosalicylaldiminate)zinc complexes cleanly exchange both ligands with rhodium(I) and iridium(I) chlorides, generating zinc chloride as an easily removable byproduct. Two ligands of differing steric demand were synthesized by the above templated route, one from 2,6-diisopropylaniline (prepared as L^1_2Zn (**1**)) and one from *p*-anisidine (prepared as L^2_2Zn (**2**)).[15] Both **1** and **2** undergo reaction with [M(cod)Cl]$_2$ to form L^1M(cod) (M = Rh (**3**), Ir (**4**)) and L^2M(cod) (M = Rh (**5**), Ir (**6**)[16]) in isolated yields ranging from 27% to 96%. All are stable, slightly air-sensitive solids which decompose in solution upon extended exposure to ambient atmosphere. The solids can be stored indefinitely under inert atmosphere and at ambient temperature. NMR spectra of each show only a single species present in solution that displays C_s symmetry. The solid-state structures of **4**, **5** and **6** were determined by X-ray diffraction analysis and are shown in Figures 2−4.[17]

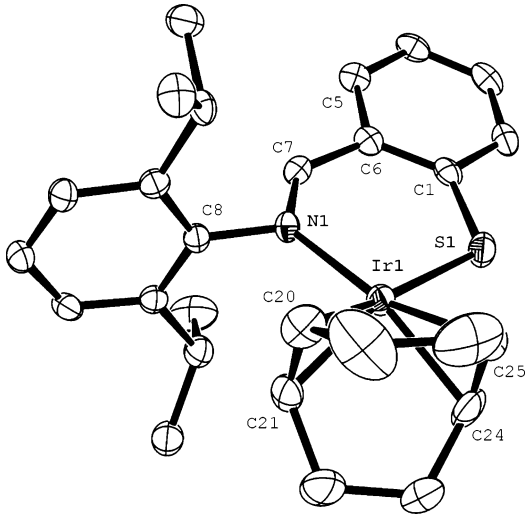

Figure 2. ORTEP diagram of **4** at 50% probability (H atoms omitted for clarity). Selected bond lengths (Å) and angles (deg): Ir1−S1, 2.275(1); Ir1−N1, 2.081(3); Ir1−C20, 2.141(4); Ir1−C21, 2.149(4); Ir1−C24, 2.148(4); Ir1−C25, 2.138(5); S1−C1, 1.730(4); N1−C7, 1.304(5); C6−C7, 1.436(5); S1−Ir1−N1, 92.74(8); N1−C7−C6−C5, 173.7(4).

The monomeric nature of complexes **4**, **5**, and **6** is somewhat surprising, given the tendency of sterically unencumbered aryl sulfides to bridge two metal centers through the sulfur atom.[18] This structural feature is particularly noteworthy given the

(10) (a) Fallon, G. D.; Nichols, P. J.; West, B. O. *J. Chem. Soc. Dalton Trans.* **1986**, 2271−2276; (b) Marini, P. J.; Murray, K. S.; West, B. O. *J. Chem. Soc. Dalton Trans.* **1983**, 143−151; (c) Marini, P. J.; Murray, K. S.; West, B. O. *J. Chem. Soc., Chem. Commun.* **1981**, 726−728.

(11) Akine, S.; Nabeshima, T. *Inorg. Chem.* **2005**, *44*, 1205−1207.

(12) Corrigan, M. F.; Rae, I. D.; West, B. O. *Aust. J. Chem.* **1978**, *31*, 587−594.

(13) (a) Frydendahl, H.; Toftlund, H.; Becher, J.; Dutton, J. C.; Murray, K. S.; Taylor, L. F.; Anderson, O. P.; Tiekink, E. R. T. *Inorg. Chem.* **1995**, *34*, 4467−4476; (b) Other methods available, see Garnovskii, A. D.; Nivorozhkin, A. L.; Minkin, V. I. *Coord. Chem. Rev.* **1993**, *126*, 1−69.

(14) Olekhnovich, L. P.; Kurbatov, V. P.; Osipov, O. A.; Minkina, L. S.; Minkin, V. I. *J. Gen. Chem. USSR* **1968**, *38*, 2512.

(15) An iron complex of L^2 has previously been prepared; see ref. 10b.

(16) Ir(cod)$_2$Cl was used as the iridium source in our reported synthetic procedure, giving identical results.

(17) Due to the number of structures present in this report, comments will be made only on structural features pertinent to this study. CIF-format files for all structures can be found in the Supporting Information.

(18) Duff, S. E.; Barclay, J. E.; Davies, S. C.; Hitchcock, P. B.; Evans, D. J. *Eur. J. Inorg. Chem.* **2005**, 4527−4532.

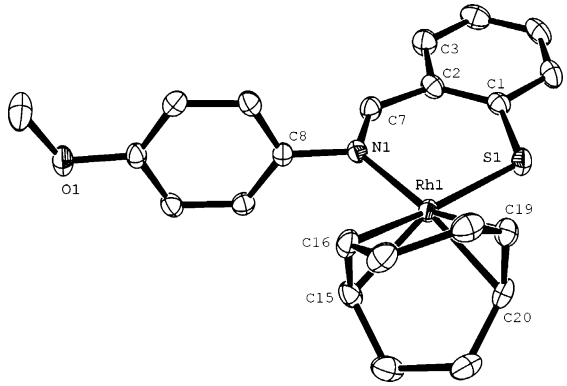

Figure 3. ORTEP diagram of **5** at 50% probability (H atoms omitted for clarity). Selected bond lengths (Å) and angles (deg): Rh1−S1, 2.2755(6); Rh−N1, 2.098(2); Rh1−C15, 2.160(2); Rh1−C16, 2.175; Rh1−C19, 2.147(2); Rh1−C20, 2.165(2); S1−C1, 1.727(2); N1−C7, 1.311(3); C2−C7, 1.436(3); S1−Rh1−N1, 92.68(5); N1−C7−C2−C3, 178.8(2).

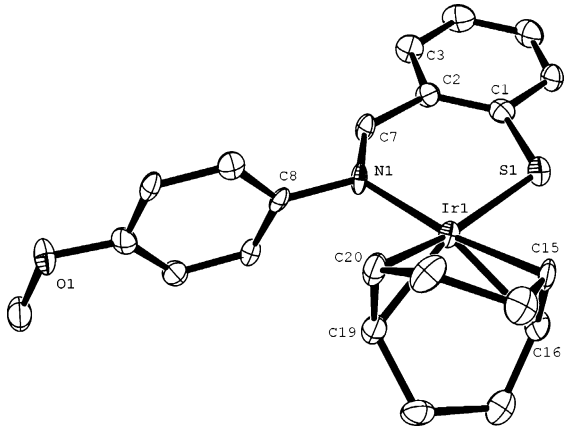

Figure 4. ORTEP diagram of **6** at 50% probability (H atoms omitted for clarity). Selected bond lengths (Å) and angles (deg): Ir1−S1, 2.268(2); Ir1−N1, 2.077(7); Ir1−C15, 2.146(9); Ir1−C16, 2.133(9); Ir1−C19, 2.141(9); Ir1−C20, 2.162(9); S1−C1, 1.734(9); N1−C7, 1.32(1); C2−C7, 1.45(1); S1−Ir1−N1, 93.5(2); N1−C7−C2−C3, 177.8(10).

absence of any sterically demanding substituents on L^2. The ligand backbone in each structure is essentially planar, with the metal lying close to this approximate plane. In the case of **6**, the greatest deviation from the least-squares plane defined by the iridium center and the atoms making up the chelate ring is 0.033(9) Å. Compound **4** displays a slight bending of the iridium center out of the plane defined by the chelate ring, a distortion common among complexes containing π-conjugated chelating ligands such as β-diketiminates.[19] The thiophenoxy-imine C−C bond lengths of **4**, **5**, and **6** are 1.436(5), 1.436(3), and 1.448(10) Å, respectively. These are contracted relative to those of a carbon−carbon single bond and thus are consistent with the conclusion that L^1 and L^2 behave as rigid, π-conjugated ligands.

2. Reaction of Iridium Complexes with Trimethylphosphine. Attempts to exchange the coordinated cod ligands on **4** or **6** with trimethylphosphine did not yield the expected bisphosphine complexes. Treatment of **4** or **6** with excess trimethylphosphine at room temperature resulted in the immediate formation of yellow solutions having ^{1}H NMR spectra consistent with the coordination of two geometrically equivalent phosphine ligands. Surprisingly, no free cod is observed. Instead, resonances exist that correspond to symmetrically bound cod (eq 2). These cod resonances are quite broad, suggesting fluxional

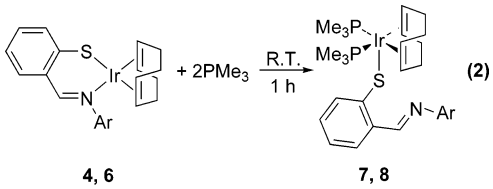

behavior at ambient temperature. The products arising from **4** and **6** were therefore assigned the formulas L^1Ir(cod)$(PMe_3)_2$ (**7**) and L^2Ir(cod)$(PMe_3)_2$ (**8**), respectively. Proton-decoupled ^{31}P NMR spectra show only a single phosphine resonance for each species. The structural motif that is most consistent with these data is a square pyramidal geometry with two phosphine ligands and cod occupying the basal positions and the thiolate sulfur occupying the apical position. Thus the thiosalicylaldiminate ligand is probably bound in a monodentate fashion.

Phosphine complex **8** decomposed to a complex mixture of unidentified compounds over a period of about 1 day in benzene solution or upon attempted isolation. While **7** was equally unstable, its decomposition products were **4** (regenerated) and the new phosphine-containing compound **9**. Heating a mixture of **4** and **9** for 30 min in the presence of added trimethylphosphine resulted in the clean conversion of the remaining **4** to **9**. Heating a mixture of **4** and three equivalents of the phosphine also cleanly generated **9**. Compound **9** exhibits an ^{1}H NMR signal consisting of an apparent doublet of triplets centered at −10.75 ppm (J = 156 Hz, 18.2 Hz) that we attributed to a metal hydride species. The absence of a signal for an imine proton suggested that site as the source of the hydride. Proton and proton-decoupled ^{31}P NMR spectra are consistent with the presence of three nonequivalent phosphine ligands. These data support the assignment of **9** as the iridium(III) species (L^1-H)-Ir$(PMe_3)_3$H where L^1-H is the product of oxidative addition of the imine C−H bond of L^1 to the iridium(I) center of intermediate **7** (eq 3). It is likely that **8** also undergoes this

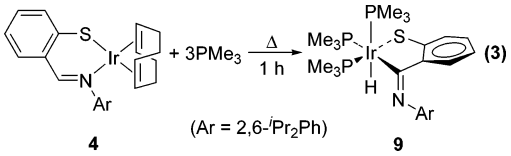

transformation, but the presumed iridium(III) product apparently reacts further to generate the complex mixture observed.

Structural elucidation of **9** by X-ray diffraction analysis confirmed the assignment made on the basis of spectroscopic data. The structure depicted in Figure 5 possesses a distorted octahedral geometry, with the atoms of the first coordination sphere bent toward the site occupied by the hydride ligand (not located). The P1−Ir1−P2 and P1−Ir1−P3 bond angles of 96.69(5) and 100.35(5)°, respectively, illustrate this distortion. The L^1-H chelate backbone is approximately coplanar with the plane defined by Ir1, S1, and C7. The orientation of the *N*-aryl ring explains the presence of two sets of isopropyl resonances in the ^{1}H NMR spectra of **9**. One isopropyl group is oriented near the phosphine ligand containing P1, rendering its two methyl groups diastereotopic. The other is situated relatively far from the sterically nondemanding hydride ligand. This effectively results in a local mirror symmetry and thus its methyl substituents are spectroscopically equivalent. Rotation around the N−Ar bond is apparently slow on the NMR time scale.

(19) (a) Nikiforov, G. B.; Roesky, H. W.; Magull, J.; Labahn, T.; Vidovic, D.; Noltemeyer, M.; Schmidt, H. G.; Hosmane, N. S. *Polyhedron* **2003**, *22*, 2669−2681; (b) Basuli, F.; Bailey, B. C.; Tomaszewski, J.; Huffman, J. C.; Mindiola, D. J. *J. Am. Chem. Soc.* **2003**, *125*, 6052−6053.

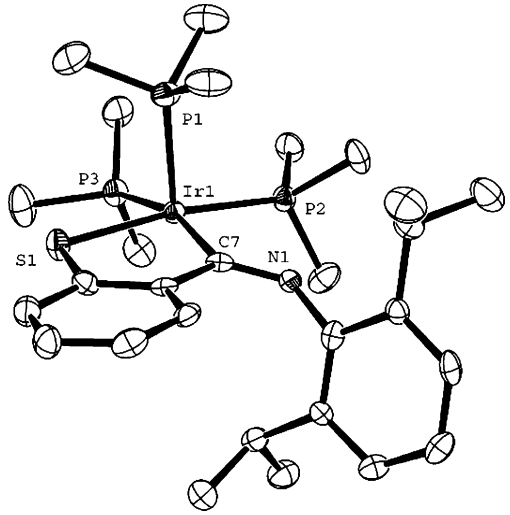

Figure 5. ORTEP diagram of **9** at 50% probability (H atoms omitted for clarity). Hydride not located. Selected bond lengths (Å) and angles (deg): Ir1−S1, 2.380(1); Ir1−P1, 2.351(2); Ir1−P2, 2.288(1); Ir1−P3, 2.337(2); Ir1−C7, 2.097(5); S1−C1, 1.736(5); S1−Ir1−P1, 90.07(5); S1−Ir1−P2, 171.68(5); S1−Ir1−P3, 87.84-(5); S1−Ir1−C7, 84.2(1); P1−Ir1−P2, 96.69(5); P1−Ir1−P3, 100.35(5); P1−Ir1−C7, 94.1(1).

Scheme 3

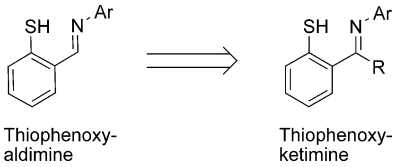

3. Preparation of Thiophenoxyketimines. The observed proclivity toward imine C−H bond insertion of the thiosalicylaldiminates prompted us to explore derivatives of this ligand architecture which might be less prone to unwanted reactivity with the metal center. The most obvious derivatization is replacement of the aldimine hydrogen with a methyl group, affording the simplest ketimine (Scheme 3). To our knowledge only a few previous examples of this ligand class exist, all being of the tetradentate type prepared by templated routes discussed previously.[20] We found that the ketimines derived from sterically unhindered anilines can be prepared directly and in good yield if the reaction mixtures are kept at ambient temperature. Compounds L^3H (**10**, Ar = *p*-C_6H_4Me) and L^4H (**11**, Ar = *p*-C_6H_4OMe) are bright red, crystalline solids that are stable in the solid state and in solution provided they are stored under inert atmosphere. Like the free thiosalicylaldimines that have been successfully isolated,[12] they display extremely downfield-shifted thiol resonances in their ^1H NMR spectra (17.3 and 18.2 ppm, respectively) which are substantially outside of the typical diamagnetic region.

X-ray diffraction studies on a sample of **10** revealed that the thiol proton is associated with the imine nitrogen, and the structure is better classified as intermediate between a thiolate zwitterion and a thioketone (Figure 6). This configuration had previously been proposed for the free thiosalicylaldimines based on spectroscopic data.[21] Iminium hydrogen H1 was located and its positional coordinates refined, while the other hydrogen atoms were placed in calculated positions. The C1−C2, C5−C6, and C1−C6 bond lengths are 1.418(3), 1.407(3), and 1.444-(3) Å, respectively. These bond lengths are considerably greater than those of a completely delocalized phenyl ring, which in this structure average 1.388 Å for the N1-bound aryl ring. The C2−C3 and C4−C5 bond lengths are significantly contracted (1.360(3) and 1.371(3) Å, respectively) and the C1−S1 bond length of 1.739(2) Å is somewhat short, lending support for contribution of the thioketone resonance form. The iminium−thiolate backbone is essentially planar, with a greatest deviation of 0.012(2) Å (C7) from the least-squares plane defined by S1, C1, C6, C7, and N1. The N1-bound aryl group is rotated by 49.5(3)° with respect to this plane and thus is out of conjugation with the rest of the π-electron system.

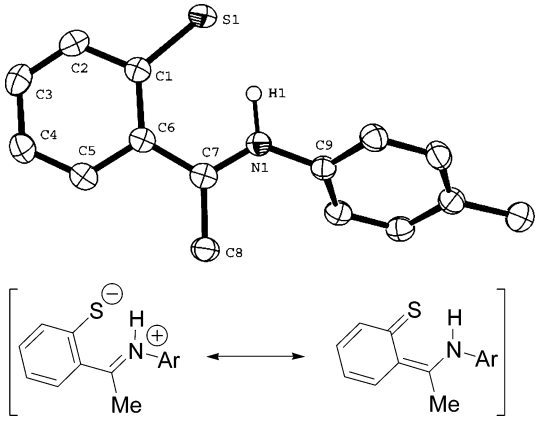

Figure 6. ORTEP diagram of **10** at 50% probability level. Calculated H atoms omitted for clarity. Selected bond lengths (Å) and angles (deg): S1−C1, 1.739(2); N1−H1, 1.04(3); N1−C7, 1.308(3); C1−C2, 1.418(3); C2−C3, 1.360(3); C3−C4, 1.398(3); C4−C5, 1.371(3); C5−C6, 1.407(3); C1−C6, 1.444(3); C6−C7, 1.456(3); S1−C1−C2, 117.0(2); S1−C1−C6, 126.5(2); C5−C6−C7−C8, 0.2(3); C7−N1−C9−C14, 49.5(3).

4. Synthesis of Thiophenoxyketimine Complexes. The alkali metal salts of L^3 (generated in situ from **10**) reacted with a variety of metal halides to form the corresponding thiophenoxyketimine complexes. Complexes of formulas $L^3M(cod)$ (M = Rh (**12**), Ir (**13**)) and $L^3M(PPh_3)_nX$ (M = Ni, X = Br, n = 1 (**14**); M = Pt, X = Cl, n = 1 (**15**), 2 (**16**)) were prepared from $[M(cod)Cl]_2$ and $(Ph_3P)_2MX_2$, respectively. The iridium system yielded multiple products when the reaction was scaled past 50 mg of **10**. However, when $Ir(cod)_2Cl$ was used in place of $[Ir(cod)Cl]_2$ the reaction proceeded to high yield (by NMR) on a 200 mg scale although separation of $L^3Ir(cod)$ (**13**) from the small percentage of byproducts drastically reduced the isolated yield. The known compound $Ir(cod)_2Cl$ exists as a mixture of $[Ir(cod)Cl]_2$ and free cod in THF solution, hence the increase in selectivity must be due in some way to the presence of the additional free cod. Stabilization of a reactive intermediate during the ligand substitution process is a possible explanation for this observation.

In the case where M = Ni, one phosphine ligand was cleanly displaced by L^3 to produce $L^3Ni(PPh_3)Br$ (**14**) quantitatively. However, incomplete phosphine displacement was observed with the platinum analogue, resulting in an equilibrium mixture of $L^3Pt(PPh_3)Cl$ (**15**) and $L^3Pt(PPh_3)_2Cl$ (**16**). In the case of **16**, L^3 is presumably bound only through the thiophenylate sulfur. The proposed structure is analogous to that bearing a similar ligand which was crystallographically determined (see below). Reasonably pure **16** was isolated by concentrating a THF solution of the crude mixture in the presence of excess triphenylphosphine (analytically pure samples could not be obtained; NMR spectra are available as Supporting Information)

(20) (a) Karsten, P.; Strahle, J. *Acta Crystallogr. Sect. C: Cryst. Struct. Commun.* **1999**, *C55*, 488−489; (b) Coombes, R. C.; Costes, J. P.; Fenton, D. E. *Inorg. Chim. Acta* **1983**, *77*, L173−L174.

(21) Corrigan, M. F.; West, B. O. *Aust. J. Chem.* **1976**, *29*, 1413−1427.

Scheme 4

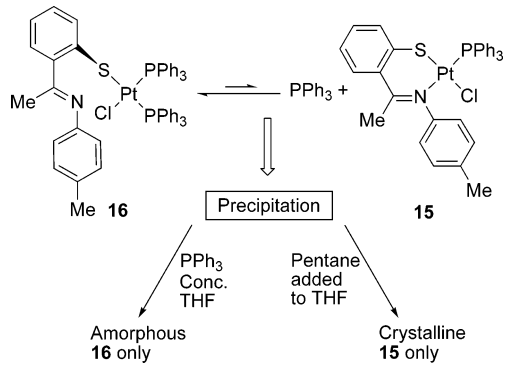

(Scheme 4). While heating resolvated **16** generated only a small amount of **15**, slow crystallization from the crude mixture (by pentane vapor diffusion) yielded crystalline **15** only. This observation suggests that crystal packing forces are sufficient to offset the energy increase in forming **15**. Surprisingly, pure **15** was also prepared by repeatedly washing solid **16** with Et_2O. The use of platinum starting materials containing more easily displaced ligands resulted only in intractable mixtures: no desired product was observed when $(PhCN)_2PtCl_2$ or $(Me_2S)_2PtCl_2$ were treated with L^3Na.

When L^4 was employed in place of L^3, a mixture of mono- and bis-phosphine complexes was again isolated. However, when $(Ph_3P)_2PtCl_2$ was treated with L^4Na at −78 °C under extremely dilute conditions (2.5 mM), $L^4Pt(PPh_3)Cl$ (**17**) and triphenylphosphine were the principal observed products. This observation implies that **17** is the kinetically favored product of this reaction, while $L^4Pt(PPh_3)_2Cl$ (**18**) and **17** are of comparable thermodynamic stability. This is puzzling if one assumes the reaction proceeds via salt metathesis followed by displacement of the phosphine by the imine functionality of L^4. The heterogeneous nature of the reaction mixture has so far precluded kinetic study, and thus a satisfactory explanation for this reactivity has been elusive. Interestingly, the most effective method for isolation of pure **17** was the simple addition of diethyl ether over an amorphous sample of the crude product. Over the course of several hours all amorphous material was converted to crystalline product, leaving in solution the triphenylphosphine liberated during the reaction. The lattice energy gained apparently drives the transformation from amorphism to crystallinity through the small equilibrium concentration of dissolved product.

Compounds **12**−**15** and **17** are stable, crystalline materials that were unchanged after exposure to air for weeks in the solid state. In solution, no decomposition was observed over several months in the absence of oxygen. No ligand disproportionation was observed when nickel complex **14** was heated at 75 °C in benzene for 24 h; thus it appears that thiophenoxyketimines do afford substitutionally inert ligands. With this in mind we wished to prepare hydrocarbyl nickel complexes that might be reactive toward olefins. However, treatment of $(Ph_3P)_2NiPhCl$ with alkali metal salts of L^3 resulted only in intractable tars. There is evidence in the literature that aryl substituents on group 10 metals can reductively couple with aryl sulfides.[22] The coupling product was not observed in the product mixture, although this decomposition pathway cannot be ruled out, as this particular diaryl sulfide might react further with the highly reactive zerovalent nickel species generated by the coupling reaction.

(22) (a) Mann, G.; Baranano, D.; Hartwig, J. F.; Rheingold, A. L.; Guzei, I. A. *J. Am. Chem. Soc.* **1998**, *120*, 9205−9219; (b) Osakada, K.; Maeda, M.; Nakamura, Y.; Yamamoto, T.; Yamamoto, A. *J. Chem. Soc. Chem. Commun.* **1986**, 442−443.

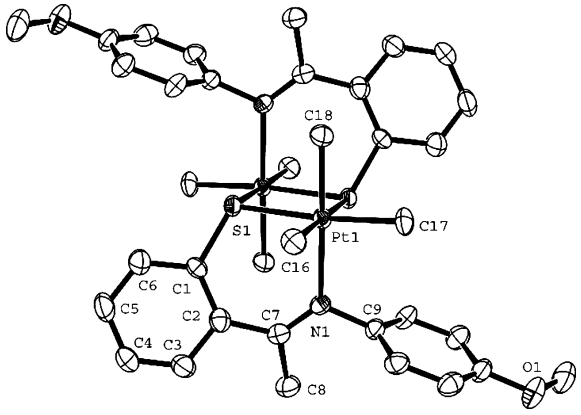

Figure 7. ORTEP diagram of **19** at 50% probability level. H atoms omitted for clarity. Selected bond lengths (Å) and angles (deg): Pt1−S1, 2.391(1); Pt1−N1, 2.198(4); Pt1−C16, 2.060(5); Pt1−C17, 2.071(5); Pt1−C18, 2.052; S1−C1, 1.754(5); C2−C7, 1.490-(7); S1−Pt1−N1, 89.6(1); S1−Pt1−C16, 95.1(2); S1−Pt1−C17, 174.5(2); S1−Pt1−C18, 89.4(2); N1−Pt1−C18, 178.4(2); C3−C2−C7−C8, 32.5(7).

In order to verify that classical organometallic complexes bearing thiophenoxyketimine ligands can exist, alkyl substituents were then investigated. Attempted alkylations of **14** with MeLi, MeMgBr, or Me_2Zn all resulted in decomposition to intractable material. This route seems to be generally avoided with respect to the salicylaldiminate complexes, suggesting a lack of compatibility with the ligand's imine fragment. Due to the comparatively facile synthesis of alkylplatinum starting materials, these were chosen for subsequent study. The reaction of $(Ph_3P)_2PtMeCl$ with L^3Na yielded multiple uncharacterized species. While heating $(Ph_3P)_2PtMe_2$ in the presence of **10** or **11** resulted only in the decomposition of the ligand, $(nbd)PtMe_2$ (nbd = norbornadiene) reacted with **11** at ambient temperature in acetonitrile (eq 4), spontaneously precipitating a modest yield

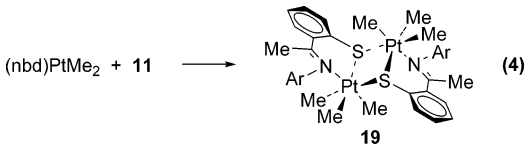

of an impure material formulated as L^4PtMe_3 (**19**) on the basis of ^1H NMR spectra (available as Supporting Information). Purification of this material has proven problematic, and thus the complex is not fully characterized.

A few high-quality crystals of **19** formed when the reaction mixture was allowed to stand, and this material was subjected to X-ray crystallographic analysis. Complex **19** is a centrosymmetric dimer wherein each sulfur atom bridges both platinum centers and each imine nitrogen binds to one of the two platinum centers (Figure 7). Interestingly, **19** is a structural analogue of the known salicylaldiminate complex formulated as $[(salnr)PtMe_3]_2$.[23] The geometry about the platinum(IV) center is only slightly distorted from the idealized octahedron. The Pt−Pt separation is 3.68 Å. Unlike the thiosalicylaldiminate complexes described above, the chelating ligand backbone is nonplanar with a twist about the C2−C7 bond of 32.5(7)°. The C2−C7 bond length is 1.490(7) Å which is significantly longer than the analogous bond length of 1.456(3) Å in the free ligand **10**.

(23) Hall, J. R.; Swile, G. A. *Aust. J. Chem.* **1975**, *28*, 1507−1511.

Scheme 5

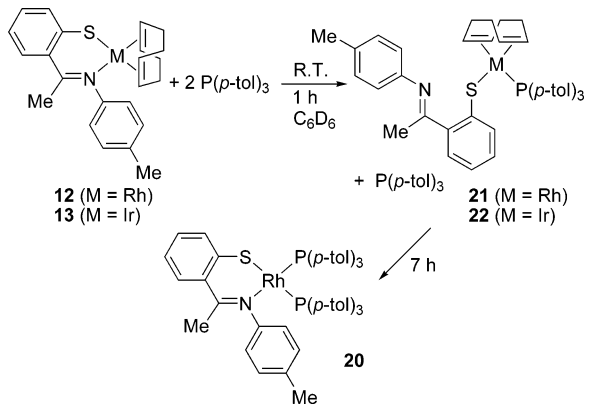

Thus the imine moiety and the thiophenylate ring are extensively deconjugated. The platinum-bound methyl group containing C17 is situated over the nitrogen-bound aryl ring. The close proximity of these two substituents apparently prevents rotation about the N1−C9 bond, which explains the observation that all of the aryl proton resonances (for each asymmetric unit) in the ^{1}H NMR spectrum of **19** are nonequivalent.

5. Reactivity of a Triarylphosphine with Thiophenoxyketimine Complexes 12, 13. Rhodium complex **12** reacted cleanly with two equivalents P(*p*-tol)$_3$ to form L^{3}Rh(P(*p*-tol)$_3$)$_2$ (**20**) over 8 h (Scheme 5). Monitoring the reaction by ^{1}H NMR (C_6D_6) revealed that no **12** was left in solution after 1 h. In addition to **20** and free cod, a third species was present in solution that gave rise to olefinic cod resonances at 5.09 and 3.45 ppm, one of which was significantly shifted relative to that of **12** (4.64 and 3.45 ppm). Proton-decoupled ^{31}P NMR spectra of the mixture show resonances corresponding to **20**, free P(*p*-tol)$_3$, and a doublet (J_{P-Rh} = 153.9 Hz) consistent with a monophosphine rhodium complex. These data are consistent with an intermediate wherein one phosphine is bound to rhodium with retention of the cod ligand. The downfield cod resonance is significantly upfield-shifted relative to free cod (5.58 ppm), indicating that both olefinic moieties are still bound to rhodium. Thus the intermediate is assigned as L^{3}Rh(cod)P(*p*-tol)$_3$ (**21**) where L^3 is bound only through the thiolate sulfur.

Complex **22**, the iridium analogue of **21**, was observed after 1 h in C_6D_6 and was the only species present in solution (other than 1 equiv of free P(*p*-tol)$_3$). Olefinic resonances in the ^{1}H NMR spectra occur at 5.07 and 3.89 ppm (compared with 4.54 and 3.05 ppm for **13**). Phosphorus NMR spectra display only two resonances in a one-to-one ratio, one corresponding to free P(*p*-tol)$_3$ and the other occurring at 22.10 ppm. No final product analogous to **20** was observed after allowing the reaction to proceed for 48 h. While this species appeared stable in solution at ambient temperature, heating or attempted isolation yielded intractable material.

The hemilabile nature of L^3 indicates that this ligand behaves more like a thiophenylate ligand with a tethered imine fragment than a rigid, conjugated ligand such as a β-diketiminate. The instability of the ligand toward alkylating agents supports this conclusion, as the alkylation of β-diketiminate-bearing complexes is a well-known transformation.[24] Therefore we wished to investigate structural aspects of these complexes that may impart the observed reactivity.

6. Crystallographic/Computational Analysis of Ligand Conformation. Several species bearing chelating L^3 or L^4 were subjected to X-ray crystallographic analysis, confirming the structural assignments made by spectroscopic means. All are square planar complexes with unremarkable bond lengths and angles around the metal centers. The nickel-containing species **14** is slightly distorted toward a tetrahedral conformation. Representative structures are depicted in Figures 8−10 (see Schemes 4 and 5 for line drawings).

The most striking feature revealed by X-ray crystallographic investigation is the lack of ligand planarity observed for the ketimine complexes. Whereas the solid-state structures of the

(24) Budzelaar, P. H. M.; van Oort, A. B.; Orpen, A. G. *Eur. J. Inorg. Chem.* **1998**, 1485−1494.

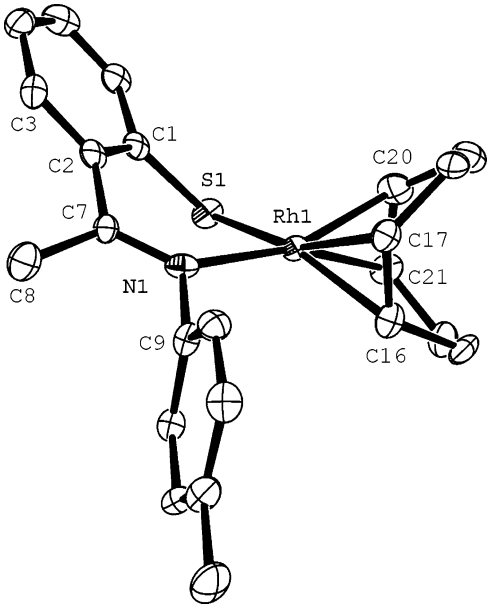

Figure 8. ORTEP diagram of **12** at 50% probability. One of two molecules in the asymmetric unit displayed. H atoms omitted for clarity. Selected bond lengths (Å) and angles (deg): Rh1−S1, 2.314(2); Rh1−N1, 2.145(5); Rh1−C16, 2.183(7); Rh1−C17, 2.163(6); Rh1−C20, 2.125(7); Rh1−C21, 2.128(6); S1−C1, 1.744(6); N1−C7, 1.307(8); C2−C7, 1.477(9); S1−Rh1−N1, 88.2(1); C3−C2−C7−C8, 35.0(7).

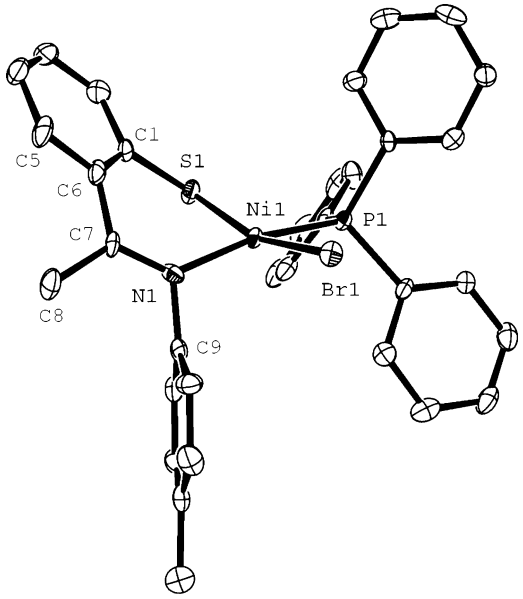

Figure 9. ORTEP diagram of **14** at 50% probability. H atoms omitted for clarity. Selected bond lengths (Å) and angles (deg): Br1−Ni1, 2.362(1); Ni1−S1, 2.149(2); Ni1−P1, 2.184(2); Ni1−N1, 1.911(5); S1−C1, 1.759(7); N1−C7, 1.284(8); C6−C7, 1.473(9); Br1−Ni1−P1, 89.50(6); Br1−Ni1−N1, 93.8(2); S1−Ni1−P1, 90.77(7); S1−Ni1−N1, 89.9(2); C5−C6−C7−C8, 27.3(9).

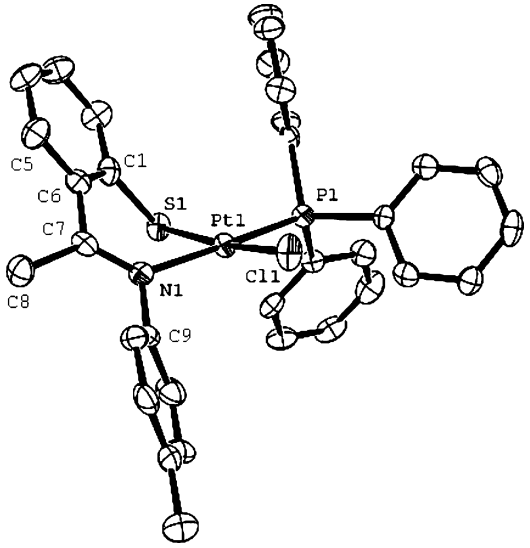

Figure 10. ORTEP diagram of **15** at 50% probability. H atoms omitted for clarity. Selected bond lengths (Å) and angles (deg): Pt1−Cl1, 2.333(2); Pt1−S1, 2.283(2); Pt1−P1, 2.220(2); Pt1−N1, 2.101(5); S1−C1, 1.779(7); N1−C7, 1.293(8); C6−C7, 1.473(9); Cl1−Pt1−P1, 95.42(6); Cl1−Pt1−N1, 89.4(1); S1−Pt1−P1, 88.25-(6); S1−Pt1−N1, 87.0(1); C5−C6−C7−C8, 37.3(9).

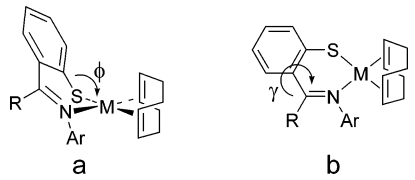

Figure 11. a. Side view of $L^RM(cod)$ defining ϕ, the cant between aryl ring and metal coordination plane. b. Top view defining γ, the torsion (twisting) angle between aryl ring and imine moiety.

aldimine complexes **4**, **5**, and **6** display approximate C_s symmetry with the metal and chelating ligand backbone defining the mirror plane, the ketimine analogues possess an extremely nonplanar ligand conformation. In these structures the thiolate phenyl ring is sharply canted with respect to the plane containing the metal and atoms of the first coordination sphere ($\phi \ll 180°$, Figure 11a). The carbon−carbon bond connecting the thiophenylate moiety with the imine fragment is twisted, bringing the imine π-bond out of conjugation with the thiophenylate ($\gamma \gg 0°$, Figure 11b). The apparent lack of π-electron conjugation may account for the reactivity trends discussed above. This geometry is observed in the solid-state structures of some nickel thiosalicylaldiminate complexes; however, there appears to be no trend in substitution pattern that would explain why some are planar and some twisted.[8b,25] Thus it appears that in those reported systems the lack of planarity is due primarily to crystallographic packing forces.

We wished to investigate, by computational methods, the source of the large differences in ligand conformation when seemingly minor structural modifications are introduced. This knowledge could then be used to ascertain whether a ketimine could be synthesized that would have the planar, conjugated conformation of the aldimines without the unwanted reactivity of the aldimine C−H bond. While energies predicted by DFT are often inaccurate compared to more sophisticated (and costly) ab initio methods, calculated geometries have been shown to

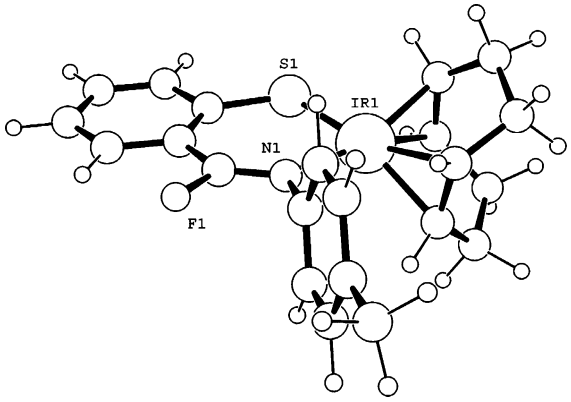

Figure 12. ORTEP diagram of $L^RIr(cod)$ where R = F. Optimized structure at B3LYP/LACVP** level of theory.

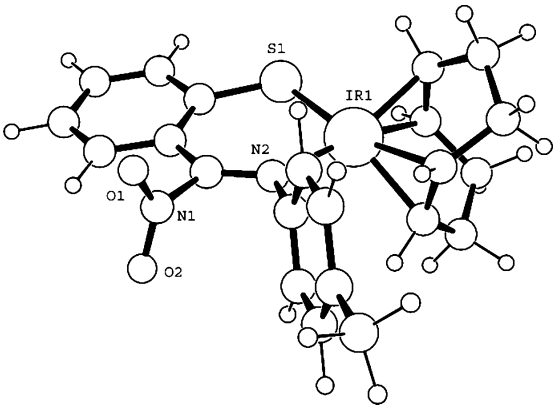

Figure 13. ORTEP diagram of $L^RIr(cod)$ where R = NO_2. Optimized structure at B3LYP/LACVP** level of theory.

agree very well with experiment.[26] Because the most obvious difference between the aldimines and ketimines is the increased steric demand of the alkyl group, our investigation focused primarily on geometry changes with varying imine substituent size. All calculations were performed at the hybrid B3LYP/LACVP** level of theory in the gas phase. As a starting point, the structures of the crystallographically determined aldimine and ketimine complexes were optimized and were found to agree well with the experimentally observed structures.

Next, the structures of the rhodium and iridium aldimine complexes were reoptimized after replacing the imine hydrogen atom with several different substituents of intermediate steric demand. The substituents chosen were fluoro, nitro, and phenyl, under the assumption that the flat π-electron system of the latter two would be oriented normal to the plane of the ligand backbone. The optimized structures of $L^RIr(cod)$ where R = F and NO_2 are shown in Figures 12 and 13, respectively. The geometries are discussed in more detail below, but one can see that in the case where R = NO_2, the plane defined by the atoms of R is approximately perpendicular to the ligand backbone.

Because the ligands in question contain an unsaturated (imine) fragment that can exist in conjugation with the thiophenylate π-electron system, one would expect that there should be resistance to breaking this conjugation. Therefore, little deviation from planarity should be observed until the steric situation becomes sufficiently problematic that ligand twisting is then favorable. After this point, π-electron conjugation is lost and the ligand is free to adopt the most favorable conformation based solely on sterics. That is, while the ligand twist angle γ (Figure

(25) (a) Bouwman, E.; Henderson, R. K.; Powell, A. K.; Reedijk, J.; Smeets, W. J. J.; Spek, A. L.; Veldman, N.; Wocadlo, S. *J. Chem. Soc. Dalton Trans.* **1998**, *3495*−3499; (b) Christensen, A.; Jensen, H. S.; McKee, V.; McKenzie, C. J.; Munch, M. *Inorg. Chem.* **1997**, *36*, 6080−6085.

(26) Guner, V.; Khuong, K. S.; Leach, A. G.; Lee, P. S.; Bartberger, M. D.; Houk, K. N. *J. Phys. Chem. A* **2003**, *107*, 11445−11459.

Table 1. Computed[a] and Experimental Ligand Torsion Angles[b] in L^RM(cod). Entries from Crystallographically Determined Structures Bear Compound Numbers in Boldface

entry	Ar	R	M	γ (deg)
1	*p*-C_6H_4Me	H	Ir	0.6
2(5)	*p*-C_6H_4OMe	H	Rh	1.2
3	*p*-C_6H_4Me	H	Rh	1.3
4(6)	*p*-C_6H_4OMe	H	Ir	2.1
5	*p*-C_6H_4Me	F	Ir	3.7
6	*p*-C_6H_4Me	F	Rh	5.2
7(4)	*p*-2,6-$^i Pr_2Ph$	H	Ir	6.2
8	*p*-C_6H_4Me	NO_2	Ir	7.1
9	*p*-C_6H_4Me	NO_2	Rh	19.4
10	*p*-C_6H_4Me	Ph	Ir	26.3
11	*p*-C_6H_4Me	Me	Ir	30.7
12(13)	*p*-C_6H_4Me	Me	Ir	33(1)
13	*p*-C_6H_4Me	Me	Rh	33.8
14	*p*-C_6H_4Me	Ph	Rh	34.6
15(12)	*p*-C_6H_4Me	Me	Rh	35.0(7)

[a] B3LYP/LACVP**. [b] See Figure 11b for definition of γ.

11) is a function of the steric extent of R, it is not a linear relationship but a step function.

Table 1 summarizes the results of the computational study, which agree reasonably well with the predictions stated above. Only a slight perturbation in geometry was observed where R = F (entries 5, 6). An increase in γ accompanies replacement of R with NO_2, especially in the case of M = Rh (entry 9) where γ is approximately two-thirds of the value for the methyl ketimine complexes. In the cases where R = Ph (entries 10, 14), the γ parameters reach values comparable to those of the methyl ketimine complexes, and thus the proposed barrier to ligand twisting has been surpassed. Therefore, this study predicts that the π-electron extent (normal to the plane containing the atoms) of a nitro group is the size limit for any substituent R, and anything larger will cause the ligand to adopt a nonplanar, twisted conformation. It should be noted that this size limit depends somewhat on the metal size, as a contraction of the N−S distance could make room for a larger R. However, further studies indicated that only in the extreme case where M = H (the free ligand) does this effect result in a planar methyl ketimine. It follows that there is unlikely to be a synthetically accessible thiophenoxyketimine that would exhibit a planar conformation upon complexation with a transition metal.

Given that the methyl ketimine complexes prefer a twisted ligand conformation, they should either have C_1 symmetry in solution or undergo a ring flip with some activation barrier. Computations on **12** indicate that this barrier should be small, with a planar configuration approximately 5 kcal/mol (not ZPE-corrected) higher in energy than that of the twisted conformation. At ambient temperature or above, ^{1}H NMR spectra of **12** and **13** exhibit somewhat broad, featureless cod resonances (Figure 14). These resonances sharpened upon cooling, resolving into complex multiplets that may result from overlapping of non-equivalent peaks (which would be the case for a C_1-symmetric complex). The peak broadening is decidedly small, but is not surprising given the minor change in electronic environment that the cod protons would experience during the ring inversion process. This broadening was not observed in spectra of the analogous (planar) aldimine complexes, a result which supports the conclusion that it is due to a facile ring inversion. Despite efforts to model this process by DFT, no planar transition state was located using several methods. It is unclear whether this is due to an extremely shallow potential energy surface or the presence of a multistep pathway for ring inversion.

7. Preparation and Structures of 3,5-Bis(trifluoromethyl)-phenyl Ketimine Complexes. Of the various ligand architectures investigated computationally, no synthetically feasible ketimine was predicted to bind in a planar conformation. We wondered if a highly electron-deficient arene might possess a sufficiently contracted π-electron cloud that it could be used in place of a nitro group, yielding a planar-binding ligand. Thus, an aryl ketimine containing a 3,5-bis(trifluoromethyl)phenyl moiety was synthesized. The aryl ketone precursor was prepared in a manner analogous to that used for 2-mercaptobenzaldehyde (Scheme 6). Thiocresol was deprotonated with *n*-butyllithium and treated with Weinreb amide **23**. The resulting ketone (**24**) was converted to ketimine ligand L^5H (**25**) in good yield by treatment with *p*-toluidine in benzene at ambient temperature. This ligand exhibited reactivity toward metal-complex precursors similar to that of the methyl ketimine analogs discussed above. Thus, $L^5Ni(PPh_3)_2Br$ (**26**), $L^5Pt(PPh_3)_2Cl$ (**27**), and $[L^5Rh(cod)]_2$ (**28**) were prepared by treatment of the appropriate metal complex with L^5K which was generated in situ from **25** (Scheme 7).

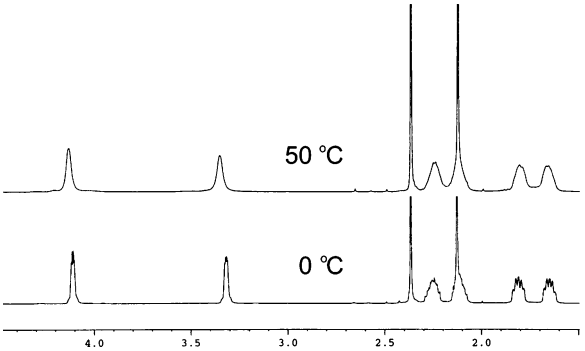

Figure 14. Selected region of the ^{1}H NMR spectrum (ppm) of **12** in CD_2Cl_2, showing broadened cod resonances at 50 °C. Ligand methyl resonances truncated.

Scheme 6

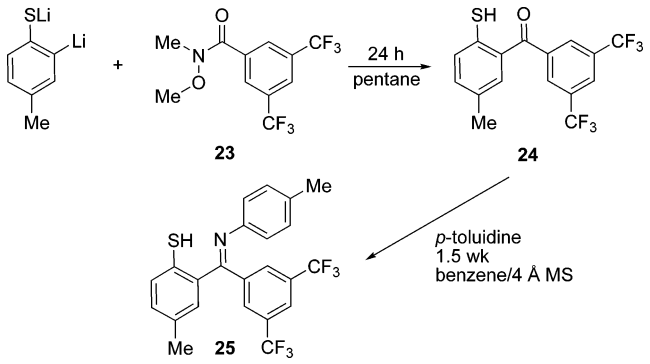

The solid-state structure of **26** depicted in Figure 15 shows a twisted ligand conformation similar to those of the methyl ketimine complexes. This datum is inconclusive with respect to the conformational study (see above), as even the nickel aldimine complexes display a variability in ligand conformation. The more informative structures would be the platinum and rhodium complexes. However, unlike the platinum systems containing L^3 or L^4, crystallization of the crude product did not yield $L^5Pt(PPh_3)Cl$. Instead, both phosphine ligands were retained as shown in Figure 16.

X-ray structural investigation of **28** revealed that it is a C_2-symmetric dimer in the solid state, with the thiolate sulfur atoms bridging the rhodium centers (Figure 17). The imine functionalities are both uncoordinated. In solution, **28** is apparently in fast exchange with its monomer and displays highly temperature-dependent NMR resonances (spectra available in Supporting

Table 2. Crystallographic Data for Compounds 4−6, 9, 10, 12−15, 19, and 26−28

compd no.	**4**	**5**	**6**	**9**	**10**
space group	$P2_1/n$	$P\bar{1}$	$P\bar{1}$	$P\bar{1}$	$P2_12_12_1$
a, Å	14.4457(9)	8.9880(6)	8.9758(7)	9.4131(7)	7.5851(5)
b, Å	11.3894(7)	10.3914(7)	10.4233(8)	11.4413(9)	11.2611(7)
c, Å	15.7491(9)	11.1130(7)	11.0658(9)	15.924(1)	14.9642(9)
α, deg	90	94.331(1)	93.684(1)	94.483(1)	90
β, deg	112.433(1)	103.799(1)	104.019(1)	89.982(1)	90
γ, deg	90	105.673(1)	106.112(1)	113.337(1)	90
V, Å^3	2395.1(3)	959.6(1)	955.3(1)	1568.9(2)	1278.2(1)
Z	4	2	2	2	4
ρ_{calcd}, g cm^{-3}	1.655	1.569	1.887	1.517	1.254
μ(Mo Kα), mm^{-1}	5.691	1.007	7.127	4.503	0.229
no. rflns measd	12110	5260	4892	8900	7021
no. indep rflns	3446	3160	2643	4336	1444
R_{int}	0.024	0.016	0.038	0.025	0.014
R_1, wR_2[a] (all)	0.0285, 0.0280	0.0261, 0.0311		0.0378, 0.0337	0.0323, 0.0433
R_1, wR_2 (obsd[b])	0.0215, 0.0263	0.0233, 0.0305	0.0383, 0.0485	0.0291, 0.0324	0.0310, 0.0431

compd no.	**12**	**13**	**14**	**15**	**19**
space group	$P2_1/c$	$P2_1/c$	$Pbcn$	$P2_1/n$	$P2_1/c$
a, Å	18.801(1)	18.850(2)	22.475(2)	12.0768(8)	8.2563(6)
b, Å	19.655(1)	19.622(2)	14.050(1)	14.864(1)	21.618(2)
c, Å	10.9890(6)	11.0043(9)	17.948(2)	17.228(1)	9.9255(7)
α, deg	90	90	90	90	90
β, deg	106.274(1)	106.214(1)	90	110.004(1)	96.223(1)
γ, deg	90	90	90	90	90
V, Å^3	3898.1(4)	3908.4(5)	5667(1)	2906.0(3)	1761.2(2)
Z	8	8	8	4	4
ρ_{calcd}, g cm^{-3}	1.538	1.838	1.503	1.676	1.873
μ(Mo Kα), mm^{-1}	0.988	6.964	2.253	5.051	8.055
no. rflns measd	17237	16864	25445	13161	8876
no. indep rflns	5274	4300	2868	3517	2538
R_{int}	0.036	0.053	0.077	0.047	0.023
R_1, wR_2 (all)	0.0655, 0.0980	0.0689, 0.0470	0.1213, 0.0955	0.0585, 0.0533	0.0324, 0.0330
R_1, wR_2 (obsd)	0.0524, 0.0853	0.0353, 0.0384	0.0510, 0.0500	0.0334, 0.0375	0.0229, 0.0298

compd no.	**26**	**27**	**28**
space group	$P2_1/c$	$P(-1)$	$C2/c$
a, Å	13.5569(9)	13.492(1)	26.474(1)
b, Å	14.7725(9)	14.743(1)	9.4643(5)
c, Å	22.151(2)	15.712(1)	26.832(1)
α, deg	90	109.336(2)	90
β, deg	91.618(1)	102.825(1)	118.924(1)
γ, deg	90	109.274(2)	90
V, Å^3	4434.4(5)	2583.9(4)	5884.2(5)
Z	4	2	4
ρ_{calcd}, g cm^{-3}	1.454	1.552	1.579
μ(Mo Kα), mm^{-1}	1.486	2.920	0.713
no. rflns measd	22642	15022	15000
no. indep rflns	5358	6612	4220
R_{int}	0.039	0.036	0.020
R_1, wR_2 (all)	0.0652, 0.0537	0.0574, 0.0465	0.0375, 0.0427
R_1, wR_2 (obsd)	0.0396, 0.0476	0.0376, 0.0417	0.0309, 0.0416

[a] $R_1 = \Sigma||F_o| - |F_c||/\Sigma|F_o|$; $wR_2 = [\Sigma\{w(F_o^2 - F_c^2)^2\}/\Sigma w(F_o^2)^2]^{1/2}$. [b] $I > 3.00\sigma(I)$.

Information). All ^{1}H NMR resonances are broad, and only a single broad peak is observed in the olefinic region. At −80 °C, this region displays many peaks. It is not clear whether these belong to the dimer and monomer or whether more than one isomer of the dimer are present. The broad olefinic peak observed at ambient temperature began to decoalesce into two peaks at 70 °C, presumably belonging to the monomer.

From these data it appears that the electron-withdrawing capabilities of the 3,5-bis(trifluoromethyl)phenyl fragment render the imine nitrogen a poor donor relative to its methyl ketimine analogues. This decrease in donor ability forces the ligand to adopt alternative coordination modes when bound to the heavier platinum group metals. Whether or not the arene substituent is sufficiently compact to allow for planar ligand binding, the observed conformational flexibility of L^5 probably precludes its use as a *β*-diketiminate analogue.

Conclusion

This paper describes a rational synthesis of thiosalicylaldiminate complexes containing heavy platinum group metals. The ligands were prepared using zinc as a template and metal chlorides were treated with the resulting complexes to yield the target species in moderate to good yield. The iridium complexes were found to undergo insertion of the metal center into the imine C−H bond in the presence of strong donor ligands.

The thiophenoxyketimines synthesized in this study display unexpected coordination behavior and in the solid state adopt twisted conformations when bound to a metal. This twisting apparently reduces *π*-electron conjugation of the thiophenylate fragment with the imine functionality. A computational study predicted that all synthetically accessible thiophenoxyketimines would be too sterically demanding to allow a planar conforma-

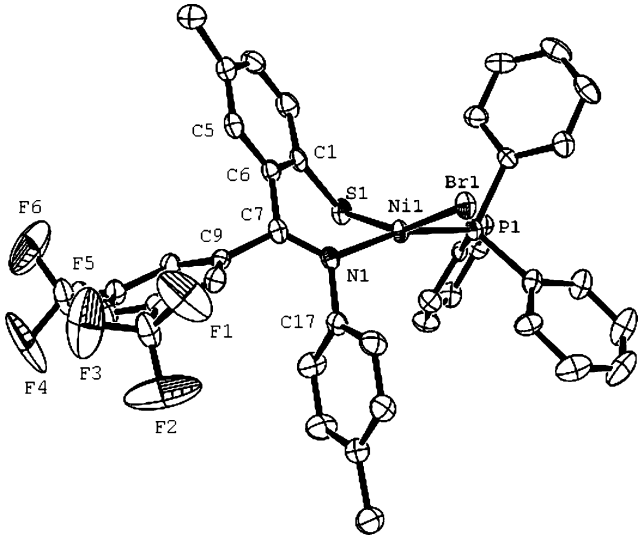

Figure 15. ORTEP diagram of **26** at 50% probability. H atoms omitted for clarity. Selected bond lengths (Å) and angles (deg): Ni1−Br1, 2.3554(6); Ni1−S1, 2.169(1); Ni1−P1, 2.157(1); Ni1−N1, 1.940(3); S1−C1, 1.777(4); N1−C7, 1.283(5); C6−C7, 1.464-(5); Br1−Ni1−P1, 90.21(3); Br1−Ni1−N1, 96.98(9); S1−Ni1−P1, 90.67(4); S1−Ni1−N1, 89.42(10); C5−C6−C7−C9, 41.6(5).

Scheme 7

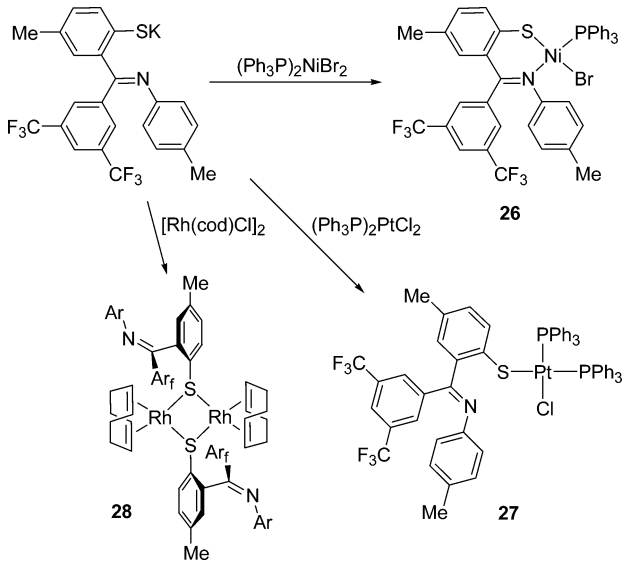

tion when metal-bound. In agreement with the computational results, the reaction chemistry of these species indicates that their behavior is consistent with the lack of a rigid, conjugated ligand backbone. As imines are generally comparatively poor ligands for heavy, soft metal centers it is therefore of little surprise that the imine functionality of this ligand class should be easily displaced by strongly binding ligands such as phosphines. A corollary to this argument is that the imine substituent would be expected to be much more susceptible to nucleophilic attack than one that is part of a conjugated system such as a β-diketiminate. The synthetic strategies now in place will facilitate investigations into the catalytic utility of this ligand class.

Experimental Section

General. All manipulations were performed using standard Schlenk-line techniques or an N_2-atmosphere glove box. Reactions followed by NMR spectroscopy were performed in 5 mm Pyrex

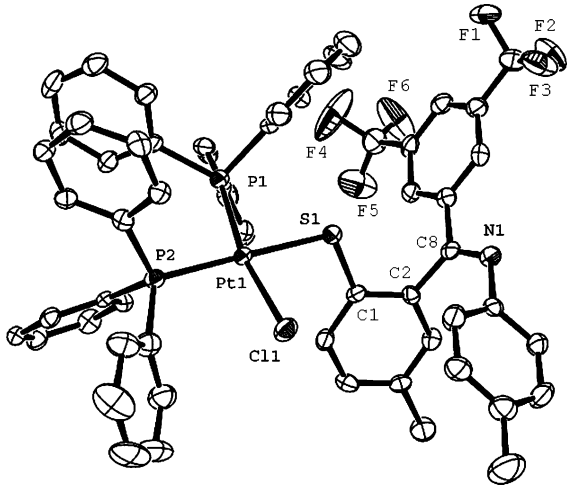

Figure 16. ORTEP diagram of **27** at 50% probability. H atoms omitted for clarity. Selected bond lengths (Å) and angles (deg): Pt1−Cl1, 2.338(1); Pt1−S1, 2.362(2); Pt1−P1, 2.253(2); Pt1−P2, 2.281(2); S1−C1, 1.757(6); N1−C8, 1.278(7); C2−C8, 1.503(8); Cl1−Pt1−S1, 88.07(5); Cl1−Pt1−P2, 90.51(5); P1−Pt1−P2, 98.58(6); P1−Pt1−S1, 82.77(5).

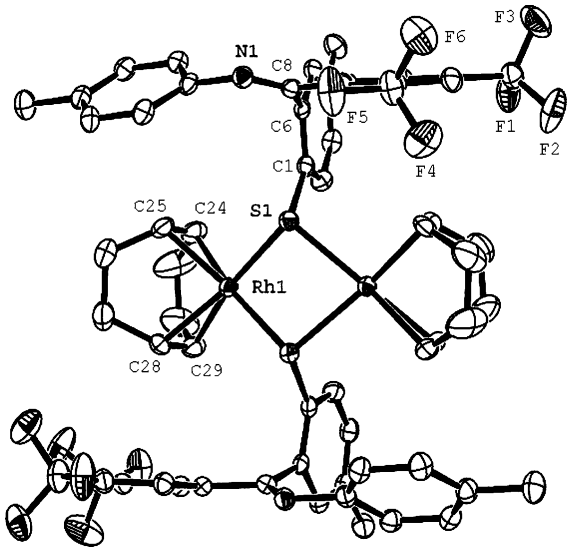

Figure 17. ORTEP diagram of **28** at 50% probability. H atoms omitted for clarity. Selected bond lengths (Å) and angles (deg): Rh1−S1, 2.3887(8); Rh1−S1′, 2.3801(8); Rh1−C24, 2.147(3); Rh1−C25, 2.148(3); Rh1−C28, 2.140(3); Rh1−C29, 2.137(3); S1−C1, 1.791(3); N1−C8, 1.273(4); C6−C8, 1.510(4); S1−Rh1−S1′, 80.64(3); Rh1−S1−Rh1′, 94.19(3).

NMR tubes which were then flame-sealed under reduced pressure. Solvents were dried by passage through a column of activated alumina,[27] degassed with nitrogen, and stored over 4 Å molecular sieves. Nonchlorinated solvents were tested with Na/benzophenone prior to use. Deuterated solvents were vacuum-transferred from Na/benzophenone, except CD_2Cl_2 and $CDCl_3$ which were vacuum-transferred from CaH_2. Molecular sieves were activated by heating at 250 °C under high vacuum for 2 d. NMR spectra were obtained with Bruker AMX-300, AMX-400, or DRX-500 spectrometers. Chemical shifts were calibrated relative to residual solvent peaks or external standards and are reported relative to TMS (^{1}H, ^{13}C), 85% H_2PO_4 (^{31}P), and $CFCl_3$ (^{19}F). Infrared spectra were recorded neat on a Thermo Nicolet Avatar 370 spectrometer equipped with a Smart Performer ATR crystal. Elemental analyses were performed

(27) Alaimo, P. J.; Peters, D. W.; Arnold, J.; Bergman, R. G. *J. Chem. Ed.* **2001**, *78*, 64.

at the UC, Berkeley Microanalytical Facility with a Perkin-Elmer 2400 Series II CHNO/S Analyzer. All starting materials obtained from commercial sources were used without further purification. 2-Mercaptobenzaldehyde[28] and its sodium salt,[29] copper *tert*-butyl sulfide,[30] $[Ir(cod)Cl]_2$,[31] $[Rh(cod)Cl]_2$,[32] $(nbd)PtMe_2$,[33] $(Ph_3P)_2PtMe_2$,[34] $(Me_2S)_2PtCl_2$,[35] $(Ph_3P)_2PtMeCl$,[36] and $(Ph_3P)_2NiPhCl$[37] were prepared according to literature procedures. $Ir(cod)_2Cl$ was prepared by cooling a concentrated solution of $[Ir(cod)Cl]_2$ in neat cod.[38]

Representative Procedure for X-ray Crystallography. A crystal of appropriate size was mounted on a glass fiber or Kaptan loop using Paratone-N hydrocarbon oil. The crystal was transferred to a Siemens SMART or APEX diffractometer/CCD area detector,[39] centered in the beam, and cooled by a nitrogen flow low-temperature apparatus that had been previously calibrated by a thermocouple placed at the same position as the crystal. Preliminary orientation matrices and cell constants were determined by collection of 60 10-s frames, followed by spot integration and least-squares refinement. An arbitrary hemisphere of data was collected and the raw data were integrated using SAINT.[40] Cell dimensions reported were calculated from all reflections with $I > 10\ \sigma$. The data were corrected for Lorentz and polarization effects, but no correction for crystal decay was applied. Data were analyzed for agreement and possible absorption using XPREP.[41] An empirical absorption correction based on comparison of redundant and equivalent reflections was applied using SADABS.[42] The structure was solved and refined with teXsan software package.[43] ORTEP diagrams were created using ORTEP-3 software package.[44]

Computational Methods. All calculations were performed using the Jaguar 5.5 package[45] with Maestro as the graphical user interface.[46] The hybrid DFT functional B3LYP[47] was used throughout, which consists of the Becke three-parameter functional[48] and the correlation functional of Lee, Yang, and Par.[49] The LACVP** basis set was employed,[50] which uses an effective core potential and valence double-ζ contraction basis functions for metals. The remaining atoms are treated with Pople's 6-31G** basis set,[51] which includes a set of *d* polarization functions for non-hydrogen atoms and a set of *p* polarization functions for hydrogens. This level of theory was sufficient to provide optimized structures that agreed quite well with those determined experimentally. All optimized structures converged well employing the DIIS convergence scheme with default convergence criteria. Increasing the size of the SCF grids and the accuracy of the numerical integrations from the default values did not have a significant effect on the optimized geometries. Vibrational frequencies were calculated for all converged structures, and their character as energy minima were confirmed by the absence of negative (imaginary) frequencies. Graphical representations of all computed structures were generated using ORTEP-3. In order to check for the presence of a planar structure as a local energy minimum in the case of the methyl ketimine complexes, the geometry of **12** was first optimized with the ligand backbone and metal-chelate ring constrained in a planar conformation. The constraints were then removed, and the optimization was performed once again. A twisted structure identical to that previously calculated was obtained, suggesting that there is no energy minimum at the planar geometry. When the optimized structure of **12** was modified such that the imine methyl group was replaced by a hydrogen atom, reoptimization of that structure yielded a planar geometry. Thus, the aldimine and ketimine complexes should each possess only one minimum-energy ligand conformation.

Selected Specific Experimental Procedures. For reasons of space, procedures in close analogy with those listed below (or are not of central importance to the discussion) are present only in the Supporting Information.

2′-*tert*-Butylsulfanylacetophenone. A Schlenk flask was charged with 2′-iodoacetophenone (5.00 g, 20.3 mmol, 1.00 equiv) and copper *tert*-butyl sulfide (3.90 g, 25.5 mmol, 1.26 equiv) and flushed with nitrogen gas. Anhydrous DMF (100 mL) was then added via cannula, and the reaction mixture was heated at 100 °C for 12 h with stirring in the absence of light. The resulting black solid was allowed to settle and the pale yellow solution decanted into a separatory funnel containing 100 mL of H_2O under ambient atmosphere. The gray, opaque suspension was extracted with Et_2O (6×50 mL). The Et_2O extracts were then combined, washed with H_2O (4×100 mL), and dried over $MgSO_4$. Filtration and removal of the solvent in vacuo yielded a light yellow oil of high purity (4.08 g, 19.6 mmol, 97%). ^1H NMR (300 MHz, $CDCl_3$): δ 7.57 (m, 1H), 7.37 (m, 3H), 2.63 (s, 3H), 1.23 (s, 9H). $^{13}C\{^1H\}$ NMR (100.6 MHz, $CDCl_3$): δ 204.90, 148.66, 138.86, 129.74, 129.12, 128.99, 127.05, 47.65, 32.26, 31.03. IR (cm^{-1}): 1693 (s), 1584 (w). Anal. Calcd. for $C_{12}H_{16}OS$: C, 69.19; H, 7.74. Found: C, 68.96; H, 7.69.

***o*-Mercaptoacetophenone.** A Schlenk flask was charged with 4.40 g (33.0 mmol, 1.00 equiv) of $AlCl_3$ under nitrogen atmosphere and suspended in 80 mL of toluene. The flask was cooled in an IPA/dry ice bath, and a solution of 2′-*tert*-butylsulfanylacetophenone (4.00 g, 19.2 mmol, 0.582 equiv) in 20 mL of toluene was added via cannula. The reaction mixture was allowed to warm to ambient temperature and was stirred for 20 h. Water (100 mL) was added to the orange suspension, and the mixture was transferred to a separatory funnel under ambient atmosphere. Extraction caused the mixture to become colorless. The organic layer was extracted with 5% aqueous NaOH (4×50 mL). All aqueous extracts were then combined and acidified with concd HCl. The resulting white suspension was extracted with Et_2O (4×50 mL), and the Et_2O extracts were combined, washed with H_2O (2×50 mL), and dried over $MgSO_4$. Filtration and removal of the solvent in vacuo resulted

(28) Still, I. W. J.; Natividad-Preyra, R.; Toste, F. D. *Can. J. Chem.* **1999**, *77*, 113−121.
(29) Kagano, H.; Itsuda, H.; Yoshida, K.; Nakano, M. (Sumitomo Seika KK, Japan). Jpn. Kokai Tokkyo Koho 05246981, 1993.
(30) Adams, R.; Reifschneider, W.; Ferretti, A. *Org. Synth.* **1962**, *42*, 22−25.
(31) Herde, J. L.; Lambert, J. C.; Senoff, C. V. *Inorg. Synth.* **1974**, *15*, 18−20.
(32) Giordano, G.; Crabtree, R. H. *Inorg. Synth.* **1979**, *19*, 218−220.
(33) Appleton, T. G.; Hall, J. R.; Williams, M. A. *J. Organomet. Chem.* **1986**, *303*, 139−149.
(34) Chatt, J.; Shaw, B. L. *J. Chem. Soc.* **1959**, 705−716.
(35) Roulet, R.; Barbey, C. *Helv. Chim. Acta* **1973**, *56*, 2179−2186.
(36) (a) Adapted from Puddephatt, R. J.; Thompson, P. J. *J. Chem. Soc. Dalton Trans.* **1977**, *1219*−1223; (b) Spectra match Davies, J. A.; Eagle, C. T.; Otis, D. E.; Venkataraman, U. *Organometallics* **1989**, *8*, 1080−1088.
(37) Hidai, M.; Kashiwag.T.; Ikeuchi, T.; Uchida, Y. *J. Organomet. Chem.* **1971**, *30*, 279−282.
(38) Onderdelinden, A. L.; Van der Ent, A. *Inorg. Chim. Acta* **1972**, *6*, 420−426.
(39) *SMART: Area-Detector Software Package*; Bruker AXS: Madison, WI, 2001−2003.
(40) *SAINT: SAX Area Detector Integration Program*, version 6.40; Bruker AXS: Madison, WI, 2003.
(41) *XPREP*, version 6.12; part of the SHELXTL Crystal Structure Determination Package; Bruker AXS: Madison, WI, 2001.
(42) *SADABS: Bruker-Nonius Area Detector scaling and Absoption Correction Program*, version 2.05; Bruker AXS: Madison, WI, 2003.
(43) *teXsan: Crystal Structure Analysis Package*; Molecular Structure Corporation, 1985 & 1992.
(44) Farrugia, L. J. *J. Appl. Crystallogr.* **1997**, *30*, 565.
(45) *Jaguar*, version 5.5; Schrodinger, LLC: Portland, OR, 2003.
(46) *Maestro*, version 6.5; Schrodinger, LLC: Portland, OR, 2004.
(47) Stephens, P. J.; Devlin, F. J.; Chabalowski, C. F.; Frisch, M. J. *J. Phys. Chem.* **1994**, *98*, 11623−11627.
(48) Becke, A. D. *J. Chem. Phys.* **1993**, *98*, 5648−5652.
(49) Miehlich, B.; Savin, A.; Stoll, H.; Preuss, H. *Chem. Phys. Lett.* **1989**, *157*, 200−206.
(50) Hay, P. J.; Wadt, W. R. *J. Chem. Phys.* **1985**, *82*, 299−310.
(51) (a) Francl, M. M.; Pietro, W. J.; Hehre, W. J.; Binkley, J. S.; Gordon, M. S.; DeFrees, D. J.; Pople, J. A. *J. Chem. Phys.* **1982**, *77*, *3654*−3665; (b) Hariharan, P. C.; Pople, J. A. *Theor. Chim. Acta* **1973**, *28*, *213*−222; (c) Hehre, W. J.; Ditchfield, R.; Pople, J. A. J. *Chem. Phys.* **1972**, *56*, *2257*−2261; (d) Ditchfield, R.; Hehre, W. J.; Pople, J. A. *J. Chem. Phys.* **1971**, *54*, 724−728.

in a brown oil which was pure by ^{1}H NMR spectroscopy. Dissolution in CH_2Cl_2 and filtration through a plug of silica removed the brown color, yielding a light yellow oil of similar purity (2.61 g, 17.1 mmol, 92%). ^{1}H NMR (300 MHz, $CDCl_3$): δ 7.89 (d, J = 7.5 Hz, 1H), 7.31 (m, 2H), 7.22 (m, 1H), 4.46 (s, 1H), 2.64 (s, 3H). Proton NMR spectra match literature values.[52]

L^1_2Zn (1). Sodium 2-formylbenzenethiolate (400 mg, 2.50 mmol, 1.00 equiv) was suspended in 15 mL of THF. Solid anhydrous $ZnCl_2$ (180 mg, 1.32 mmol, 0.528 equiv) was added, and the mixture was stirred for 1 h. 2,6-Diisopropylaniline (448 mg, 2.53 mmol, 1.01 equiv) was then added, followed by 5 g of 4 Å molecular sieves. This mixture was allowed to stand for 2 d, after which time the cloudy solution was filtered and the solvent was removed under vacuum. The residue was dissolved in 5 mL of CH_2Cl_2 and filtered once more. The volume of the resultant yellow solution was reduced to 2 mL and cooled to −30 °C. The supernatant was decanted from the yellow crystalline product that had formed, and the solid was washed with Et_2O (4 × 2 mL) yielding pure **1** (581 mg, 0.882 mmol, 71%). Solvent removal from the supernatant and washes resulted in a residue which, after washing with pentane (5 × 1 mL), yielded an additional 125 mg (0.190 mmol) of **1** of sufficient purity for further use. ^{1}H NMR (500 MHz, CD_2Cl_2): δ 8.17 (s, 2H), 7.28 (br s, 2H), 7.17 (m, 6H), 6.96 (m, 4H), 6.87 (br s, 2H), 3.23 (br s, 2H), 2.67 (br s, 2H), 1.41 (br s, 6H), 1.04 (d, J = 6.5 Hz, 12H), 0.60 (br s, 6H). ^{13}C{^{1}H} NMR (125.8 MHz, CD_2Cl_2): δ 173.83, 149.39, 146.97, 142.16 (br), 139.73 (br), 137.32, 136.81, 131.78, 130.62, 127.26, 124.37 (br), 123.09 (br), 122.63, 29.52, 29.28, 25.83, 23.69, 21.64. IR (cm^{-1}): 1620, 1604, 1585, 1541. Anal. Calcd. for $C_{38}H_{44}N_2S_2Zn$: C, 69.33; H, 6.74; N, 4.26. Found: C, 68.99; H, 6.67; N, 4.11.

L^1Rh(cod) (3). A solution of **1** (200 mg, 0.304 mmol, 1.00 equiv) in 5 mL of THF was slowly added to $[Rh(cod)Cl]_2$ (150 mg, 0.304 mmol, 1.00 equiv) dissolved in 12 mL of THF. After the reaction mixture was stirred for 4 h, the solvent was removed under vacuum. The residue was extracted with Et_2O (4 × 5 mL), and the filtered extracts were combined and reduced to 10 mL. The solution was held at −30 °C for 24 h, resulting in the precipitation of 252 mg (0.496 mmol, 82%) of pure **3**. ^{1}H NMR (500 MHz, CD_2Cl_2): δ 8.19 (d, J = 2.5 Hz, 1H), 7.83 (d, J = 7.5 Hz, 1H), 7.34 (t, J = 7.5 Hz, 1H), 7.25 (m, 3H), 7.09 (t, J = 7.5 Hz, 1H), 4.48 (m, 2H), 3.49 (m, 2H), 3.35 (sept, J = 7.0 Hz, 2H), 2.32 (m, 4H), 2.02 (m, 2H), 1.90 (m, 2H), 1.40 (d, J = 7.0 Hz, 6H), 1.02 (d, J = 7.0 Hz, 6H). ^{13}C{^{1}H} NMR (125.8 MHz, CD_2Cl_2): δ 167.96, 149.82, 140.87, 138.11, 132.68, 131.93, 130.11, 127.56, 124.18, 123.90, 122.65, 86.50, 78.23, 30.96, 30.53, 28.74, 25.72, 22.63. IR (cm^{-1}): 1590, 1572, 1524. Anal. Calcd. for $C_{27}H_{34}NRhS$: C, 63.90; H, 6.75; N, 2.76. Found: C, 63.92; H, 6.55; N, 2.72.

L^2Rh(cod) (5). A solution of **2** (129 mg, 0.234 mmol, 1.00 equiv) in 5 mL of THF was slowly added to $[Rh(cod)Cl]_2$ (116 mg, 0.235 mmol, 1.00 equiv) dissolved in 10 mL of THF. After the reaction mixture was stirred for 6 h, the solvent was removed under vacuum. The residue was extracted with 3 mL of CH_2Cl_2, filtered, and heated to boiling while 2 mL of pentane was added. The vessel was then cooled to −30 °C overnight. The supernatant was decanted, and the orange solid was washed with Et_2O (3 × 1 mL) (204 mg, 0.450 mmol, 96%). Crystals suitable for X-ray diffraction analysis were grown by vapor diffusion of pentane into a solution of **5** in THF. ^{1}H NMR (500 MHz, THF-d_8): δ 8.39 (s, 1H), 7.72 (d, J = 8.0 Hz, 1H), 7.46 (d, J = 6.5 Hz, 1H), 7.22 (m, 1H), 7.07 (d, J = 8.5 Hz, 2H), 6.96 (m, 1H), 6.89 (d, J = 8.5 Hz, 2H), 4.37 (br s, 2H), 3.78 (s, methyl and cod olefinic overlapping, 5H), 2.27 (m, 4H), 1.95 (br s, 2H), 1.85 (br s, 2H). ^{13}C{^{1}H} NMR (125.8 MHz, THF-d_8): δ 168.61, 158.84, 151.46, 149.23, 138.51, 132.45, 131.43, 130.47, 125.28, 121.70, 114.25, 84.35, 76.85, 55.79, 31.36, 30.90. IR (cm^{-1}): 1605, 1590, 1574, 1523. Anal. Calcd. for $C_{22}H_{24}NORhS$: C, 58.28; H, 5.34; N, 3.09. Found: C, 58.14; H, 5.21; N, 3.15.

(L^1-H)Ir(PMe_3)$_3$H (9). Compound **4** (73.5 mg, 0.123 mmol, 1.00 equiv) was dissolved in 1 mL of benzene, and 0.70 mmol (5.7 equiv) of trimethylphosphine was added via vacuum transfer. The reaction mixture was then heated at 65 °C for 1 h. The solvent and excess phosphine were removed under reduced pressure, and the residue was dissolved in 1 mL of CH_2Cl_2. Crystalline material was obtained by slow vapor diffusion of pentane (2 mL) into the CH_2Cl_2 solution (64.5 mg, 0.0900 mmol, 73%). ^{1}H NMR (500 MHz, CD_2Cl_2) δ 7.26 (d, J = 7.0 Hz, 1H), 7.03 (m, 1H), 6.91 (m, 1H), 6.78 (m, 1H), 6.65 (m, 2H), 6.15 (t, J = 7.0 Hz, 1H), 3.27 (sept, J = 7.0 Hz, 1H), 2.91 (sept, J = 7.0 Hz, 1H), 1.76 (d, J_{H-P} = 10 Hz, 9H), 1.65 (d, J_{H-P} = 8.0 Hz, 9H), 1.36 (d, J_{H-P} = 8.5 Hz, 9H), 1.22 (d, J = 7.0 Hz, 3H), 1.13 (d, J = 7.0 Hz, 3H), 1.01 (d, J = 7.0 Hz, 3H), 0.47 (d, J = 7.0 Hz, 3H), −11.22 (d of t, J_{H-P} = 191 Hz, 22.5 Hz, 1H). ^{13}C{^{1}H} NMR (100.6 MHz, CD_2Cl_2): δ 190−185 (m), 156.66, 154.15, 151.01, 136.21, 133.86, 127.99, 127.66, 127.53, 124.38, 123.17, 120.29, 118.40, 28.44 (d, J_{C-P} = 49 Hz), 25.32 (d, J_{C-P} = 25 Hz), 23.71 (d, J_{C-P} = 36 Hz), 22.22, 21.94, 21.79, 21.42, 17.28, 17.01. ^{31}P{^{1}H} NMR (162.0 MHz, CD_2Cl_2): δ −44.65 (m), −58.58 (m), −63.80 (m). IR (cm^{-1}): 2026, 1579, 1545. Anal. Calcd. for $C_{28}H_{49}IrNP_3S$: C, 46.91; H, 6.89; N, 1.95. Found: C, 47.16; H, 6.96; N, 1.93.

L^3H (10). *o*-Mercaptoacetophenone (591 mg, 3.88 mmol, 1.00 equiv) was diluted with 15 mL of benzene and *p*-toluidine (416 mg, 3.88 mmol, 1.00 equiv) was added, followed by 5 g of 3 Å molecular sieves. The reaction mixture was allowed to stand for 2 days, during which time the solution became deep red. After solvent removal, the resulting amorphous powder was dissolved in 3 mL of THF and gently heated. During heating, pentane (15 mL) was slowly added, resulting in the formation of bright red crystals upon cooling. The reaction vessel was then placed in a −30 °C freezer overnight. The supernatant was removed, and the crystalline material (791 mg, 3.28 mmol, 84%) was washed with pentane. Note: the crude product was pure by ^{1}H NMR and could be used without purification. Crystals suitable for X-ray crystallographic analysis were grown by cooling a concentrated solution of **10** in Et_2O. ^{1}H NMR (500 MHz, CD_2Cl_2): δ 17.33 (s, 1H), 7.74 (d, J = 1.5 Hz, 1H), 7.72 (d, J = 1.0 Hz, 1H), 7.31 (d, J = 8.0 Hz, 2H), 7.13 (m, 3H), 6.98 (m, 1H), 2.55 (s, 3H), 2.41 (s, 3H). ^{13}C{^{1}H} NMR (125.8 MHz, CD_2Cl_2): δ 172.08, 162.19, 138.35, 138.32, 136.57, 131.97, 130.57, 130.53, 128.11, 124.37, 121.36, 21.37, 18.40. IR (cm^{-1}): 1615, 1585, 1531. Anal. Calcd. for $C_{15}H_{15}NS$: C, 74.65; H, 6.26; N, 5.80. Found: C, 74.47; H, 6.41; N, 5.76.

L^3Rh(cod) (12). Yellow $[Rh(cod)Cl]_2$ (203 mg, 0.412 mmol, 1.00 equiv) was dissolved in 10 mL of THF and cooled to −30 °C. Ligand **10** (200 mg, 0.829 mmol, 2.01 equiv) was dissolved in 4 mL of THF, and NaH (21.3 mg, 0.843 mmol) was added, causing vigorous gas evolution. After 30 min, the solution had become light yellow, at which time it was slowly added to the cooled $[Rh(cod)Cl]_2$ solution. The mixture was allowed to stir for 4 h, and the solvent was removed under vacuum. ^{1}H NMR spectra showed quantitative conversion to product. The residue was dissolved in 3 mL of CH_2Cl_2 and filtered, and the solution was gently heated while 10 mL of pentane was slowly added. The reaction vessel was placed in a −30 °C freezer overnight. The supernatant was removed from the resulting orange crystalline material, and the solid was washed with pentane (342 mg, 0.758 mmol, 92%). Slow evaporation of a CH_2Cl_2 solution of **12** yielded crystals of sufficient quality for X-ray diffraction analysis. ^{1}H NMR (500 MHz, CD_2Cl_2): δ 7.62 (d, J = 7.5 Hz, 1H), 7.45 (d, J = 8.0 Hz, 1H), 7.21 (d, J = 8.0 Hz, 2H), 7.08 (m, 1H), 6.99 (m, 1H), 6.91 (d, J = 8.0 Hz, 2H), 4.14 (br s, 2H), 3.35 (br s, 2H), 2.38 (s, 3H), 2.27 (br s, 2H), 2.14 (br s, methyl and cod methylene overlapping, 5H), 1.81 (br s, 2H), 1.67 (br s, 2H). ^{13}C{^{1}H} NMR (125.8 MHz, CD_2Cl_2): δ 171.42, 148.67,

(52) Topolski, M. *J. Org. Chem.* **1995**, *60*, 5588−5594.

147.40, 138.44, 135.71, 132.66, 131.26, 129.90, 129.82, 122.28, 121.84, 86.23 (d, $J_{C-Rh} = 10.1$ Hz), 76.68 (d, $J_{C-Rh} = 12.6$ Hz), 31.46, 30.59, 24.31, 21.21. IR (cm^{-1}): 1958, 1933, 1903, 1582, 1565, 1534, 1504. Anal. Calcd. for $C_{23}H_{26}NRhS$: C, 61.19; H, 5.80; N, 3.10. Found: C, 61.11; H, 5.95; N, 3.18.

$L^3Pt(PPh_3)Cl$ (15). NaH (9.98 mg, 0.416 mmol, 1.00 equiv) was added to a solution of **10** (100 mg, 0.414 mmol, 0.995 equiv) in 5 mL of THF. The mixture was stirred for 30 min and was then added dropwise to a suspension of $(Ph_3P)_2PtCl_2$ (326 mg, 0.413 mmol, 0.993 equiv) in 10 mL of THF and stirred overnight. The solvent was removed under reduced pressure, and the residue was extracted with 10 mL of benzene and lyophilized. The crude product was allowed to stand under 10 mL of Et_2O for 2 weeks, and the Et_2O was then decanted. This process was then repeated, after which time the remaining solid was extracted with 2 mL of THF. Vapor diffusion of pentane (1 mL) into this solution resulted in crystalline **15** (64.5 mg, 0.0880 mmol, 21%). ^1H NMR (500 MHz, CD_2Cl_2): δ 7.62 (m, 6H), 7.52 (d, $J = 7.0$ Hz, 1H), 7.44 (m, 3H), 7.37 (m, 6H), 7.29 (m, 5H), 7.14 (m, 2H), 2.44 (s, 3H), 2.28 (s, 3H). $^{13}C\{^1H\}$ NMR (125.8 MHz, CD_2Cl_2): δ 171.32, 146.93, 141.46 (d, $J_{C-P} = 6.3$ Hz), 136.73, 135.10 (d, $J_{C-P} = 11.3$ Hz), 132.17, 131.23, 131.15, 130.55, 130.30, 129.79, 129.42, 128.40 (d, $J_{C-P} = 11.3$ Hz), 125.13, 124.80, 23.53, 21.38. $^{31}P\{^1H\}$ NMR (162 MHz, CD_2Cl_2): δ 12.02 ($J_{P-Pt} = 3914$ Hz). IR (cm^{-1}): 1594, 1552, 1505. Anal. Calcd. for $C_{33}H_{29}ClNPPtS$: C, 54.06; H, 3.99; N, 1.91. Found: C, 53.70; H, 3.81; N, 1.82. Compound **16**, present in the crude reaction mixture, was not obtained in analytically pure form. NMR spectra of **16** are available as Supporting Information.

$[L^4PtMe_3]_2$ (19). A solution of **11** (40.0 mg, 0.155 mmol, 1.00 equiv) in 3 mL of acetonitrile was slowly added to 49.5 mg (0.156 mmol, 1.01 equiv) of $(nbd)PtMe_2$ in 5 mL of acetonitrile. The mixture quickly developed a dark orange color and then turned light orange after ca. 5 min. After 6 h, a brick red precipitate had formed which was collected by filtration and washed with acetonitrile (3 × 1 mL). This sparingly soluble material was not successfully purified although its ^1H NMR spectrum is consistent with the crystallographically determined structure (see Supporting Information). The supernatant from the reaction mixture was allowed to stand for 2 d, during which time a few high-quality crystals formed which were used for the X-ray structural determination.

$L^3Rh(P(p\text{-}tol)_3)_2$ (20). Tri(*p*-tolyl)phosphine (135 mg, 0.444 mmol, 1.00 equiv) was added to a solution of **12** (100 mg, 0.222 mmol, 0.500 equiv) dissolved in 10 mL of benzene, causing a rapid color change from orange to dark purple/red. The reaction mixture was stirred for 24 h, after which time the solvent was removed under reduced pressure. The residue was dissolved in 2 mL of THF and heated to boiling while 12 mL of hexane was slowly added. Upon cooling to ambient temperature, the vessel was cooled at −30 °C for 24 h. The supernatant was decanted, and the dark purple solid was washed with Et_2O (3 × 2 mL) (167 mg, 0.175 mmol, 79%). ^1H NMR (500 MHz, CD_2Cl_2): δ 7.64 (d, $J = 7.5$ Hz, 1H), 7.41 (m, 6H), 7.28 (d, $J = 7.5$ Hz, 1H), 7.23 (m, 1H), 7.10 (t, $J = 7.5$ Hz, 1H), 7.07 (d, $J = 8.0$ Hz, 2H), 6.90 (m, 12H), 6.80 (m, 6H), 6.35 (br s, 2H), 2.46 (s, 3H), 2.32 (s, 9H), 2.29 (s, 9H), 1.92 (s, 3H). $^{13}C\{^1H\}$ NMR (125.8 MHz, CD_2Cl_2): δ 169.75, 149.06, 146.33, 138.82, 138.66, 135.16, 135.02, 134.93, 134.69, 134.32, 134.22, 133.88, 133.58, 132.89, 130.20, 128.79, 128.06, 127.98, 127.45, 123.92, 121.82, 21.78, 21.56, 21.50, 21.29. $^{31}P\{^1H\}$ NMR (162.0 MHz, CD_2Cl_2): δ 46.51 (dd, $J_{P-P} = 42.1$ Hz, $J_{P-Rh} = 179.8$ Hz), 40.02 (dd, $J_{P-P} = 42.1$ Hz, $J_{P-Rh} = 183.1$ Hz). IR (cm^{-1}): 1598, 1578, 1539. Anal. Calcd. for $C_{57}H_{56}NP_2RhS$: C, 71.92; H, 5.93; N, 1.47. Found: C, 70.91; H, 6.02; N, 1.41. Analysis of two independently prepared and purified samples showed similarly low abundance of carbon. NMR spectra of pure **20** are available as Supporting Information.

L^5H (25). Molecular sieves (3 Å, 4.5 g), 15 mL of benzene, compound **24** (1.00 g, 2.74 mmol, 1.00 equiv), and *p*-toluidine (297 mg, 2.77 mmol, 1.01 equiv) were combined and left to stand for 10 d. The reaction mixture was then filtered away from the molecular sieves and lyophilized. The bright yellow residue was dissolved in 3 mL of Et_2O, and 5 mL of pentane was slowly added while the solution was gently heated. The vessel was then cooled to −30 °C overnight. The crystalline solid was collected via filtration and washed with pentane (6 × 1 mL), yielding 878 mg of product. The pentane washes were added to the supernatant, which upon cooling afforded an additional 126 mg of pure **25** (1.00 g total, 2.21 mmol, 81%). ^1H NMR (400 MHz, C_6D_6): δ 8.43 (s, 2H), 7.79 (s, 1H), 6.90 (d, $J = 8.0$ Hz, 2H), 6.80 (d, $J = 8.0$ Hz, 2H), 6.75 (d, $J = 8.0$ Hz, 1H), 6.51 (m, 2H), 2.80 (s, 1H), 1.91 (s, 3H), 1.71 (s, 3H). $^{13}C\{^1H\}$ NMR (100.6 MHz, C_6D_6): δ 163.24, 147.56, 141.27, 136.35, 135.62, 134.70, 132.26 (q, $J_{C-F} = 33.2$ Hz), 131.32, 130.74, 130.08, 129.54, 128.72 (d, $J_{C-F} = 3.0$ Hz), 126.67, 124.04 (quint, $J_{C-F} = 4.0$ Hz), 123.77 (q, $J_{C-F} = 273.6$ Hz), 121.22, 20.75, 20.50. ^{19}F NMR (376.5 MHz, C_6D_6): δ −61.93. IR (cm^{-1}): 2563, 1627, 1596, 1504. Anal. Calcd. for $C_{23}H_{17}F_6NS$: C, 60.92; H, 3.78; N, 3.09; S, 7.07. Found: C, 61.04; H, 3.92; N, 2.90; S, 7.40.

$[L^5Rh(cod)]_2$ (28). Potassium *tert*-butoxide (13.8 mg, 0.123 mmol, 1.00 equiv) was added to a solution of **25** (55.6 mg, 0.123 mmol, 1.00 equiv) in 3 mL of THF. After stirring for 30 min, the mixture was added dropwise to a solution of $[Rh(cod)Cl]_2$ (30.2 mg, 0.0612 mmol, 0.498 equiv) in 10 mL of THF. The reaction mixture was stirred for 3 h, after which time the solvent was removed under reduced pressure. The residue was extracted with 2 mL of benzene, and the extract was filtered into a small vessel, into which 1 mL of pentane vapor was allowed to slowly diffuse. Large crystals of [**28**·0.5 pentane] were collected and washed with Et_2O (3 × 1 mL) (56.8 mg, 0.0813 mmol, 66%). ^1H NMR spectra of **28** at three temperatures are included in the Supporting Information. These spectra, as well as the elemental analysis, were obtained using the same sample that was used for the X-ray diffraction studies. IR (cm^{-1}): 1630, 1604, 1595, 1504. Anal. Calcd. for $C_{31}H_{28}F_6NRhS\cdot 0.5C_5H_{12}$: C, 57.51; H, 4.90; N, 2.00. Found: C, 57.39; H, 5.03; N, 2.00.

Acknowledgment. We are indebted to Dr. Fred Hollander and Dr. Allen Oliver at the UC Berkeley CHEXRAY X-ray crystallographic facility and Dr. Kathleen Durkin at the Molecular Graphics Facility (NSF grant CHE-0233882) for crystallographic and computational consultation, respectively. We also thank Prof. F. Dean Toste for advice concerning ligand syntheses. This work was supported by NSF grant CHE-0345488 to R.G.B. and DOE funding to J.A.

Supporting Information Available: CIF-format files for all crystallographically determined structures, experimental procedures for compounds not listed above, NMR spectra of **16**, **19**, **20** and **28**, positional coordinates of all computed structures. This material is available free of charge via the Internet at http:/pubs.acs.org.

OM0609057